

1 **Ongoing exposure to peritoneal dialysis fluid alters resident peritoneal macrophage**
2 **phenotype and activation propensity**

3
4 **Tara E. Sutherland^{1,2,4}, Tovah N. Shaw^{1,2,3}, Rachel Lennon^{4,5}, Sarah E. Herrick^{1,5}, Dominik**
5 **Rückerl^{1*}**

6
7 1 Lydia Becker Institute for Immunology and Infection, Faculty of Biology, Medicine and Health,
8 Division of Infection, Immunity and Respiratory Medicine, University of Manchester,
9 Manchester, UK

10 2 Manchester Collaborative Centre for Inflammation Research (MCCIR), University of
11 Manchester, Manchester, UK

12 3 Institute of Immunology and Infection Research, School of Biological Sciences, University of
13 Edinburgh, Edinburgh, UK

14 4 Wellcome Centre for Cell-Matrix Research, University of Manchester, Manchester, UK

15 5 Division of Cell Matrix Biology and Regenerative Medicine, Faculty of Biology Medicine and
16 Health, School of Biological Sciences, University of Manchester, Manchester, UK

17
18 **Keywords: peritoneal dialysis, fibrosis, macrophage, inflammation, tissue resident, glucose**
19 **degradation product**

20
21 *** Correspondence:**

22 Dr. Dominik Rückerl

23 Dominik.Ruckerl@manchester.ac.uk

24
25 Word count: 6653 words

26 Figure count: 7

27
28 **Abstract:**

29
30 Peritoneal dialysis (PD) is a more continuous alternative to haemodialysis, for patients with
31 chronic kidney disease, with considerable initial benefits for survival, patient independence and
32 healthcare costs. However, longterm PD is associated with significant pathology, negating the
33 positive effects over haemodialysis. Importantly, peritonitis and activation of macrophages is
34 closely associated with disease progression and treatment failure. However, recent advances in
35 macrophage biology suggest opposite functions for macrophages of different cellular origins.
36 While monocyte-derived macrophages promote disease progression in some models of fibrosis,
37 tissue resident macrophages have rather been associated with protective roles. Thus, we aimed
38 to identify the relative contribution of tissue resident macrophages to PD induced inflammation
39 in mice. Unexpectedly, we found an incremental loss of homeostatic characteristics, anti-
40 inflammatory and efferocytic functionality in peritoneal resident macrophages, accompanied by
41 enhanced inflammatory responses to external stimuli. Moreover, presence of glucose
42 degradation products within the dialysis fluid led to markedly enhanced inflammation and almost
43 complete disappearance of tissue resident cells. Thus, alterations in tissue resident macrophages
44 may render longterm PD patients sensitive to developing peritonitis and consequently
45 fibrosis/sclerosis.

47 **Introduction:**

48

49 An estimated 5-10 million people worldwide die every year due to chronic kidney disease [1]. In
50 Europe, an average of 850 people per million population (pmp) require renal replacement therapy
51 (RRT) and 120 new patients pmp commence treatment annually [2]. The average 5-year survival
52 rate of patients receiving RRT is only 50.5%. This can be improved to over 90% if patients receive
53 a kidney transplant, but rates of transplantation remain low (32 pmp) primarily due to organ
54 availability, and the majority of patients rely on dialysis as a therapy to substitute excretory
55 kidney function [2].

56

57 Peritoneal dialysis (PD), utilizing the body's own peritoneal membrane as a filter during dialysis, is
58 a cost-effective alternative to haemodialysis (HD). Although PD has been associated with better
59 initial survival rates [3], lower costs for the health system [4] and increased patient autonomy [5]
60 as compared to HD, the incidence rate of PD over several decades has dropped in Europe [3].
61 There are a variety of reasons for this reduction in PD uptake, but the significant risk of adverse
62 effects and in some cases fatal outcomes, has limited the general adoption of PD in adult patients
63 across Europe [6]. Treatment failure is commonly associated with repeated episodes of peritonitis
64 (i.e. inflammation) and a progressive thickening and vascularisation of the peritoneum, leading to
65 impaired filtration and thus reduced efficacy of PD [6, 7]. In rare cases, the fibrotic changes to the
66 peritoneum become so extreme that they form a fibrous cocoon encapsulating the internal
67 organs, called Encapsulating Peritoneal Sclerosis (EPS), leading to persistent or recurring
68 adhesive bowel obstruction [7-9]. The diagnosis of EPS is an indication to urgently discontinue PD
69 with the mortality approaching 50% within one year after diagnosis [10]. Management of EPS
70 includes surgery but there is a relatively high frequency of symptom recurrence. In contrast,
71 immunosuppressive treatments and the use of anti-fibrotic agents, like tamoxifen, have shown
72 noticeable benefits to patient survival [10]. Therefore, aberrant activation of the immune system
73 appears to be linked to both alteration of peritoneal structure and PD treatment failure, as well as
74 the progression of the fibrotic sequelae. Indeed, experimental rodent models of the disease, have
75 suggested inappropriate or excessive activation of macrophages (M Φ) as a major cause of the
76 pathology [11-14].

77

78 Recent advances in M Φ biology have highlighted the intrinsic heterogeneity of M Φ populations
79 [15]. Grossly simplified, M Φ can be split into tissue resident macrophages (M Φ res) which are
80 present in tissues during homeostasis, and monocyte-derived macrophages (M Φ mono), which
81 are recruited to the tissue during inflammatory conditions [16]. Both M Φ populations can and do
82 respond to external stimuli, like infection, but they possess distinct response profiles and adopt
83 distinct functional properties [17, 18].

84

85 In health, peritoneal M Φ res are essential for maintaining tissue homeostasis by silently removing
86 apoptotic cells through efferocytosis [19, 20] and by providing a source of tissue-reparative cells
87 that infiltrate surrounding tissues (e.g. the liver) during injury [21]. Importantly, upon
88 encountering inflammatory signals, M Φ res undergo the Macrophage Disappearance Reaction
89 (MDR) [22]. Following injection of inflammatory agents (e.g. bacterial antigens) or infection, the
90 number of peritoneal M Φ res detectable in peritoneal lavage will drop significantly within a few
91 hours [23]. The exact mechanism underlying MDR is still not completely understood, but it has
92 been proposed that M Φ res undergo activation-induced cell death [18] or adhere to the
93 mesothelial lining of the peritoneal cavity reducing their recovery via lavage [21, 24, 25]. Of note,
94 the degree of detectable M Φ res -loss directly correlates to the amount of inflammatory stimulus
95 (e.g. cfu of bacteria) and the recruitment of inflammatory M Φ mono [18]. Following resolution of

96 inflammation, MΦres can re-populate the peritoneal cavity and return to homeostatic numbers
97 through proliferative expansion of remaining MΦres [26].

98

99 In models of fibrotic disorders of the lung or kidney, influx of monocytes and monocyte-derived
100 MΦ has been linked to disease progression and induction of pathology [27-29]. Similarly, in
101 rodent models of peritoneal fibrosis, preventing the influx of monocytes or depleting all MΦ
102 limits the degree of peritoneal thickening and improves glomerular filtration [11, 30, 31].
103 Moreover, injection of MΦmono, activated ex vivo using bacterial antigens (i.e.
104 lipopolysaccharide), often referred to as M1 MΦ, exacerbates disease progression [14]. Together
105 these data highlight a role for inflammation and infiltration of MΦmono in the progression of
106 peritoneal fibrosis and seem to provide a cohesive picture explaining the enhanced risk of PD
107 failure associated with repeated episodes of peritonitis [32]. In this context, it is interesting to
108 note that continuing peritoneal irrigation and thus continual removal of peritoneal cells, including
109 any inflammatory infiltrate, in patients discontinuing PD, has been suggested to prevent
110 subsequent EPS formation [33].

111 Other studies in rodents have found a role for anti-inflammatory, IL-4-activated MΦ (also called
112 M2), characterised by the expression of CD206, Arg1 and Ym1, in promoting peritoneal dialysis
113 fluid (PD fluid) induced fibrosis [11, 34, 35]. Additionally, chronic fibrotic kidney disease is linked
114 to a switch from inflammatory M1 to predominantly M2 activated MΦ [36]. Indeed, both types of
115 MΦ activation seem to have the capacity to promote kidney fibrosis, possibly acting during
116 different phases of the pathology [37]. Importantly, some markers used to define M2 are
117 differentially expressed on MΦres and MΦmono. For example CD206 is expressed constitutively
118 by MΦmono but not MΦres [17]. Thus, the described role of M2 MΦ may merely reflect an
119 enhanced influx of MΦmono rather than IL-4-mediated activation. In fact, transfer of
120 exogenously activated M2 MΦ showed no impact on disease progression in a model of peritoneal
121 fibrosis [14] and even reduced pathology in a model of renal fibrosis [38]. Moreover, using
122 different strategies to deplete MΦ in kidney fibrosis yielded opposing results with regard to
123 disease progression indicating that depletion of different subsets of MΦ may lead to different
124 outcomes [39]. Indeed, renal MΦres as compared to MΦmono have been shown to be protective
125 in a model of kidney pathology [29]. This suggests that the cellular origin of MΦ may play a
126 prominent part in determining their role during fibrotic disorders and influence the overall disease
127 outcome.

128

129 Here we analysed the effects of repeated PD fluid injection on MΦ population dynamics and
130 responses to activating signals. Our data indicate a significant change in MΦres phenotype over
131 time during PD fluid administration. MΦres lost expression of anti-inflammatory and efferocytic
132 markers correlating with enhanced inflammatory responses to external stimulation. Importantly,
133 the enhanced inflammatory phenotype of MΦres persisted even when PD fluid administration
134 was stopped. Interestingly, Nanostring- transcript analysis revealed reduced expression of genes
135 in the Adenosine / G-protein-receptor coupled pathway indicating a potential cause for the loss of
136 regulatory phenotype in MΦres. In contrast, addition of glucose degradation products, known
137 enhancers of PD-pathology [40], led to strongly enhanced inflammation, virtually complete loss
138 of MΦres and enhanced engagement of the TGF-β- as well as Interferon- associated pathways.
139 Thus, repeated exposure to PD fluid may render patients more susceptible to peritonitis, and by
140 extension, to peritoneal fibrosis due to exaggerated inflammatory responses.

141

142 **Results:**

143

144 **Dialysis fluid induces the disappearance of tissue resident MΦ**

145

146 To determine the impact of peritoneal dialysis fluid (PD fluid) injection on peritoneal MΦ
147 populations (see supplementary Fig S1 for gating strategy) we first characterised the cellular
148 dynamics induced after a single application of PD fluid. Six hours after PD fluid injection MΦres
149 underwent a pronounced disappearance reaction with the number of F4/80 high MΦres reduced
150 to approximately 30% of the levels found in naïve control animals (Fig 1A). Simultaneously, a
151 significant influx of neutrophils and Ly6C high monocytes were detected, indicative of an
152 inflammatory response (Fig 1B&C). Of note, similar to previous reports [23] tissue dwelling,
153 monocyte-derived MΦmono (F4/80 low MHC-II high) also underwent a disappearance reaction
154 and were reduced in numbers by approximately 40 % (Fig 1D). F4/80 high MΦres displayed
155 limited signs of activation at this early time point post PD fluid injection. No increased expression
156 of MHC-II could be detected (Fig 1E). In contrast intracellular Ym1 and CD206 expression were
157 significantly enhanced following PD fluid injection, but expression was restricted to less than 10 %
158 of cells (Fig 1F&G). The disappearance of MΦres in this context seemed in part due to enhanced
159 cell death as indicated by increased levels of Annexin V staining (Fig 1H). By 24 hours post PD
160 fluid injection, the numbers of MΦres had returned to baseline levels and expression of CD206
161 was no longer significantly different, whereas Ym1 expression remained elevated compared to
162 naïve controls (Fig S2).

163 Overall, these data are consistent with the induction of low grade inflammation caused by PD
164 fluid injection accompanied by a significant change in the prevalence of various myeloid cell
165 populations within the peritoneal cavity.

166

167 **Repeated PD fluid treatment induces a gradual change in MΦres phenotype**

168

169 We next sought to determine the long term effect of PD fluid administration on peritoneal MΦ
170 populations. For this, animals were injected once per day, 5 times a week with PD fluid i.p. and
171 the peritoneal exudate cells (PEC) analysed 24 hours after 1, 4, 9 and 14 injections, respectively
172 (Fig 2A). Over the course of the experiment the number of MΦres remained consistently lower in
173 Physioneal treated animals as compared to naïve mice (Fig 2B). Simultaneously, enhanced influx
174 of Ly6C monocytes and successive accumulation of F4/80 low MΦmono could be detected in the
175 peritoneal cavity following multiple rounds of PD fluid injection (Fig 2C& D).

176 Despite the overall reduced numbers of MΦres, repeated injection of PD fluid led to marked
177 induction of Ki67 expression in MΦres, indicative of proliferative expansion (Fig. S3). This is in line
178 with a previous report demonstrating repopulation of the peritoneal cavity by MΦres following an
179 inflammatory insult through proliferation [41]. Thus, it is likely that PD fluid injection leads to a
180 repeated cycle of MΦres disappearance followed by repopulation. Similarly, it is likely that the
181 gradual influx of monocytes and MΦmono underlies cyclic fluctuations after each round of PD
182 fluid injection. Thus, this data indicated that MΦ populations within the peritoneal cavity undergo
183 dynamic but limited changes following PD fluid instillation, with a slight accumulation of
184 MΦmono over time.

185 Closer investigation of the MΦres phenotype, however, revealed a progressive loss of
186 characteristics that define the tissue resident phenotype. In particular markers associated with
187 the efferocytic and anti-inflammatory function of MΦres were expressed at increasingly lower
188 levels following repeated injection of PD fluid (Fig 2E - G). T cell immunoglobulin and mucin
189 domain containing 4 (Tim4), a molecule associated with the efficient removal of apoptotic cells
190 [42, 43] as well as V-set and immunoglobulin domain-containing 4 (Vsig4), associated with
191 limiting inflammatory responses [44, 45], are specifically expressed in MΦres during steady state
192 conditions [46]. MΦres gradually lost expression of these markers with increasing number of PD
193 fluid injections (Fig 2 E & G). Similarly, CD73, an anti-inflammatory effector molecule specifically

194 expressed by MΦres [47, 48] was found to be significantly reduced after 14 injections of PD fluid
195 (Fig 2 F).

196 In contrast, expression of CD102 (ICAM2) was not altered by PD fluid injection (Fig 2 H). A similar
197 phenotype (loss of MΦres marker expression with sustained CD102 expression) has previously
198 been described in mice lacking the transcription factor Gata6, indicating that repeated PD fluid
199 injection may exert its effects via affecting Gata6 expression [49]. However, no significant
200 difference in Gata6 expression by MΦres was found after 9 injections of PD fluid measured in
201 subsequent experiments (Fig 2 I). Notably, Gata6 expression levels varied following PD fluid
202 injection with diminished expression detected in approximately 50 % of animals (Fig 2 I). Thus,
203 any effect of PD fluid injection on Gata6 expression may be transient or reflect the impact of
204 other factors, like the degree of inflammation.

205 Taken together, following repeated PD fluid injection, MΦres, while retaining their tissue identity
206 (F4/80 high CD102+ Gata6+), lose some of their functional characteristics and in particular anti-
207 inflammatory and efferocytosis associated functions.

209 **Repeated PBS injection but not chronic bacterial infection leads to a loss of MΦres** 210 **characteristics**

211
212 As shown in Figure 1 and previously reported [14], repeated injection of PD fluid is associated with
213 the induction of low grade inflammation as evidenced by influx of neutrophils and Ly6C+
214 monocytes. Thus, to assess whether the loss of MΦres functional markers (i.e. Tim4, CD73, Vsig4)
215 was due to the elicited inflammatory response, we analysed peritoneal exudate cells from animals
216 subjected to prolonged bacterial infection. Animals were infected orally with attenuated
217 *Salmonella enterica* ser. Typhimurium (SL3261, ΔaroA) and peritoneal cells analysed during the
218 chronic phase of infection, 34 and 55 days post infection. In line with previous data [18] and
219 confirming the inflammatory environment, MΦres from SL3261 infected animals showed clear
220 upregulation of MHC-II as well as enhanced expression of Sca-1 on day 55 (Fig 3A & B). Moreover,
221 persistent influx of neutrophils was detected in the peritoneal cavity of SL3261 infected animals
222 (Fig 3C) as well as live, cfu-forming bacteria (Fig 3D) confirming an ongoing pro-inflammatory
223 activation.

224 However, unlike following repeated PD fluid injection, MΦres isolated from animals harbouring *S.*
225 *Typhimurium* did not show any noticeable loss of Tim4, CD73 or Vsig4 expression in the chronic
226 phase of the infection (Fig 3 E-G). Rather to the contrary MΦres from SL3261 infected animals
227 expressed elevated levels of Tim4 (Fig 3 E). Thus, chronic inflammatory conditions alone did not
228 cause the progressive loss of MΦres phenotype as observed following repeated Peritoneal
229 injection. Importantly, injection of sterile PBS instead of PD fluid induced similar, albeit less
230 pronounced changes in peritoneal MΦ phenotype (Fig 4A). This would indicate that repeated
231 disturbance of the peritoneal immune system alone, rather than specific constituents of the
232 dialysis fluid, was sufficient to drive the observed alterations in peritoneal MΦres. However, PD
233 fluid enhanced these effects (Fig 4A).

234 Furthermore, it has been suggested that male peritoneal dialysis patients have a significantly
235 reduced survival rate on PD than female patients [50]. Although the reason for this discrepancy is
236 unknown and likely due to multiple factors, differences in the inflammatory response may
237 contribute to the observed effects. Moreover, male and female mice differ considerably in the
238 maintenance and cellular dynamics of peritoneal MΦ [51]. Thus, we assessed the effect of
239 repeated PD fluid injection on myeloid cell populations in male and female mice. MΦres from
240 naive male or female mice showed comparable expression levels of CD73 and Vsig4. In contrast
241 naive male mice showed considerably lower expression of Tim4 (Fig 4B-D). However,

242 independent of these differences in the steady state, Physioneal induced the loss of Tim4, CD73
243 and Vsig4 in both sexes to a similar degree.
244 Taken together this data shows that repeated disturbance of the peritoneal environment triggers
245 low grade inflammation which alters the MΦres phenotype.

246

247 **Prolonged PD fluid injection alters the response of MΦres to external stimuli**

248

249 Our previous data had highlighted a significant loss of Tim4 as well as Vsig4 and CD73, markers
250 which have been associated with MΦres core functions (i.e. efferocytosis and anti-inflammatory
251 activity) [42, 45, 52]. Thus, we next aimed to assess whether repeated injection of dialysis fluid
252 altered MΦ functional responses.

253 To test the capacity of MΦres to take up and ingest apoptotic cells, whole PEC from animals
254 injected for various times with Physioneal or from naive controls were incubated in the presence
255 of apoptotic thymocytes labelled with pHrodo. pHrodo labelled cells emit a very low, nearly
256 undetectable fluorescent signal after staining, but will become brightly fluorescent and clearly
257 detectable by flow cytometry after encountering an acidic environment, as found inside a
258 phagolysosome [53]. Thus, use of pHrodo allows the reliable detection of ingested apoptotic cells
259 as compared to labeled cells bound to the surface of a phagocyte.

260 Repeated injection of Physioneal gradually reduced the proportion of myeloid cells (total
261 CD11b+lin-) capable of ingesting apoptotic cells (Fig 5A). This was in part due to the increased
262 proportion of Ly6C high monocytes and F4/80 low, monocyte-derived MΦ within the myeloid cell
263 pool (Fig 2C&D), cells which possess reduced efferocytic activity [54]. However, when the analysis
264 was restricted to MΦres a similar progressively reduced capacity to ingest apoptotic cells was
265 detected (Fig 5B). Thus, MΦres from Physioneal injected animals seemed to lose the functionality
266 to carry out efferocytosis efficiently. Of note, this loss of efferocytic capacity was not restricted to
267 the use of dialysis fluid, as repeated injection of sterile PBS induced a similar reduction in the
268 capacity of MΦres to ingest apoptotic cells (Fig S4A).

269 To further analyse whether MΦres from Physioneal injected animals were in general less
270 responsive to external stimuli, we subjected whole PEC to in vitro stimulation with LPS and rIFN γ .
271 MΦres from PD fluid treated animals showed a gradually increasing inflammatory response
272 towards bacterial stimulation (Fig 5C&D). The proportion of cells expressing NOS2 or Sca-1,
273 markers of pro-inflammatory M1 activation [55, 56], was consistently higher in cells from PD fluid
274 treated animals as compared to cells from naive animals (Fig 5C&D). Indeed, Sca-1 was not found
275 to be upregulated on naive MΦres after 6 h stimulation with IFN γ /LPS in vitro, indicating
276 repeated Physioneal injections resulted in a stronger and more rapid response of MΦres to pro-
277 inflammatory stimuli.

278 Importantly, an enhanced activation profile was not only observed in response to pro-
279 inflammatory stimuli, but also in response to rIL-4, a driver of M2, anti-inflammatory MΦ
280 activation [57]. MΦres stimulated with rIL-4 for 24 h showed increased expression of Ym1 and at a
281 later timepoint also Relm α (Fig 5 E&F).

282 Thus, MΦres altered their functional repertoire following repeated exposure to dialysis fluid, with
283 reduced efferocytic capacity and enhanced responses to both M1 and M2 polarising stimuli.

284

285 **Altered PD fluid-induced responsiveness of MΦres is maintained after treatment is discontinued**

286

287
288 Next, we examined whether the phenotypical and functional changes observed in MΦres
289 following repeated PD fluid injection were temporary or persisted even after treatment ceased.
290 For this, mice were injected 5 times a week with Physioneal or PBS for a total of 9 injections, a

291 timepoint when the altered MΦres phenotype is evident (Fig 2), and then rested for seven days.
292 Subsequently, the PEC were collected and analysed for the expression of activation markers as
293 well as re-stimulated in vitro to analyse their response to external stimuli as described above.
294 MΦres from discontinued Physioneal or PBS injected animals maintained a reduced expression of
295 CD73, Tim4 and Vsig4 compared to naive controls (Fig 6A). Similarly, MΦres from Physioneal and
296 PBS injected animals showed an enhanced response to in vitro stimulation with LPS/IFN γ (NOS $_2$,
297 Sca1; stimulated for 6 h) (Fig 6B). To verify whether the altered MΦ phenotype observed in rested
298 MΦres was due to the integration of inflammatory, monocyte-derived cells into the resident pool
299 we conducted lineage tracing experiments using Cx3cr1^{CreER}:R26-eyfp mice [58]. Animals were
300 dosed daily during the first 5 days of the experiment with Tamoxifen by oral gavage. This method
301 will efficiently label peritoneal monocyte-derived MΦ populations (eg. MΦmono) while MΦres
302 remain unlabelled. This allows to determine the degree of integration of monocyte-derived cells
303 into a resident MΦ population [58]. In addition, all animals were treated as described above (9
304 injections of Physioneal, 5 times per week) and rested for a further seven days (Fig 6C). In our
305 hands approximately 20 % of Ly6C-CD115+ blood monocytes stained positive for eYFP two weeks
306 after the last tamoxifen administration confirming efficient labelling. Moreover, the degree of
307 labelling found in blood monocytes was independent of any treatment with Physioneal or PBS
308 (suppl. Fig S5). In contrast, approximately 2.5 % of peritoneal F4/80 high MΦres from naive
309 animals were eYFP+ (Fig 6D) confirming their maintenance is partly independent of monocytic
310 influx [59]. Animals injected with Physioneal exhibited a slightly higher proportion (~ 5 %) of
311 eYFP+ MΦres (Fig 6D), indicating enhanced integration of monocyte derived cells into the
312 resident pool. However, independent of any treatment, the proportion of eYFP+ cells in MΦres
313 did not reach the same levels as observed in F4/80 low MHC-II high MΦmono (~ 12%; Fig 6D).
314 Thus, although Physioneal treatment did increase the rate at which monocyte-derived cells
315 integrated into the MΦres pool, the population remained to a significant part resident in origin.
316 Of note, the enhancement of MΦres turnover and monocyte-integration was similarly observed
317 in PBS treated animals (Fig 6D). Importantly, MΦres from tamoxifen-treated Cx3cr1^{CreER}:R26-
318 eyfp mice showed similar behaviour in response to repeated Physioneal / PBS injection as
319 observed above, as indicated by a loss of CD73, Tim4 and Vsig4 expression (suppl. Fig S5).
320 Therefore the observed changes in MΦres phenotype can not be explained due to enhanced
321 integration of monocyte derived MΦ into the resident pool alone.
322 These data highlight that repeated PD fluid injections sensitise resident peritoneal MΦ and, thus,
323 potentially exacerbate the severity and the detrimental sequelae of peritonitis events.
324

325 **Glucose degradation products strongly enhance inflammatory responses and loss of tissue** 326 **resident MΦ markers**

327
328 Since our previous data revealed limited differences between injection of dialysis fluid and
329 injection of sterile saline solution (PBS), we wanted to verify whether addition of glucose
330 degradation products (GDP), altered the observed MΦ responses. GDP can form in dialysis fluid
331 due to the heat sterilisation process [60] and have been previously shown to strongly enhance
332 PD-associated fibrosis in humans and mice [40, 61]. Thus, animals were injected with Physioneal
333 containing 40 mM Methylglyoxal (MGO) for 14 injections and analysed 24 h after the last
334 injection. Addition of MGO to the dialysis fluid dramatically altered the immune profile of the
335 mice, leading to strongly enhanced inflammatory influx, as indicated by significantly enhanced
336 numbers of neutrophils, Ly6C+ monocytes and F4/80 low MHC-high MΦmono (Fig 7A).
337 Moreover, the loss of Tim4, CD73 and Vsig4 expression in F4/80 high (CD11b+ lineage-) cells
338 observed following Physioneal injection was even further enhanced by MGO supplementation
339 (Fig 7 C). However, although the number of cells within the F4/80 high (CD11b+ lineage -) gate

340 were not altered by the addition of MGO (Fig 7 A), these were likely not tissue-resident derived
341 MΦ as indicated by their altered flow-cytometry profile (Fig 7B), as well as the loss of CD102, a
342 marker of tissue residency in peritoneal MΦ [49], which remained unaffected by injection of
343 Physioneal alone (Fig 7C). In addition, Physioneal supplemented with MGO induced significant
344 inflammatory activation of total peritoneal myeloid cells (CD11b+ lineage- cells) as indicated by
345 enhanced expression of Sca-1 and NOS2 (Fig 7D). Furthermore, MΦ markers associated with
346 fibrosis, CD206 and Ym1, were exclusively upregulated in MGO-treated, highly inflammatory
347 settings. In contrast arginase 1 (Arg1) was upregulated in Physioneal treated animals, but not in
348 Physioneal + MGO treated animals (Fig 7 D). Thus, the presence of glucose degradation products
349 strongly enhanced the inflammatory response leading to an almost complete disappearance of
350 homeostatic MΦres.

351 To further elucidate the differences between PD-fluid alone and PD-fluid enriched with glucose
352 degradation products, we analysed gene expression of total peritoneal exudate cells using the
353 Nanostring nCounter Fibrosis panel platform. Due to legal animal welfare restrictions on the
354 maximum number of i.p. injections we were allowed to give in our experiments, we were unable
355 to detect any histological signs of fibrosis in our model (data not shown). However, in line with
356 previous publications demonstrating considerable thickening of the peritoneum within 5 - 8
357 weeks of daily PD-fluid instillation [11, 61], injection of Physioneal led to the significant up
358 regulation of a series of genes associated with ECM-remodelling and epithelial-mesenchymal
359 transition (EMT) (Fig 7 E). Moreover, in line with the low level inflammation detected by flow
360 cytometry, genes associated with cytokine & neutrophil pathways were significantly enhanced in
361 Physioneal treated animals. Of note, genes associated with the Adenosine- & G-protein coupled
362 receptor signalling pathway were significantly reduced in Physioneal treated animals (Fig 7 F) in
363 line with our finding of reduced CD73 expression (Fig 7 C). Moreover, addition of MGO led to a
364 further increase in expression of inflammatory genes and in particular Interferon-related genes
365 (Cytokine & Interferon pathways; Fig 7 G) in accordance with the enhanced influx of inflammatory
366 cells (Fig 7 A). Furthermore, co-administration of MGO also led to marked increases in expression
367 of Tgf-β-pathway associated genes (Fig 7 G), in line with the previously described enhancement
368 of fibrosis induced by glucose degradation products [61].

369 Taken together these data highlight, that the presence of glucose degradation products
370 dramatically alters the immune profile within the peritoneal cavity and that distinct gene
371 signatures are associated with steady PD-fluid instillation as compared to pathological
372 conditions.

373

374 **Discussion:**

375 MΦ are versatile cells implicated in many pathologies [62]. They play both essential protective as
376 well as detrimental / pathological roles, often within the same disease setting [63-65]. Thus, the
377 regulatory mechanisms governing MΦ responses have become the focus of current research
378 aiming to dissect these contradictory behaviours. Moreover, scientists have proposed MΦ as an
379 excellent target for therapeutic interventions, as altering their phenotype may not only improve
380 disease outcome, but actively revert associated pathologies. Here we show, that tissue resident,
381 peritoneal MΦ gradually lose their homeostatic, anti-inflammatory phenotype following PD-fluid
382 instillation and, in particular, a loss of regulation via the Adenosine pathway. In addition we show
383 that the presence of glucose degradation products, known enhancers of PD-associated pathology
384 [40], induces strong inflammatory responses characterised by enhanced Tgf-β- and Interferon
385 signalling.

386

387 Recent discoveries have highlighted the inherent diversity of the MΦ pool, indicating the
388 presence of different types of MΦ with different ontogeny [59], response profiles [17] and

389 functional roles [18]. In particular, MΦres and acutely recruited MΦmono have been identified as
390 distinct mediators of pathology. During lung fibrosis recruited MΦmono have been shown to be
391 essential drivers of the fibrotic pathology and disease progression [27]. Similarly, in murine
392 models of peritoneal dialysis associated fibrosis, infiltration of MΦmono has been shown to be
393 detrimental to disease outcome [11, 14, 30, 31]. Furthermore, significant changes in the prevalence
394 of specific MΦ/monocyte populations have been described in dialysis patients, dependent on the
395 history of peritonitis episodes [12]. Thus, the pathology inducing effect of peritonitis associated
396 inflammation in peritoneal dialysis seem to be due to the recruitment and accumulation of
397 fibrosis promoting cells like MΦmono. Similar to these findings, we observed low-grade
398 inflammation and infiltration of MΦmono in our system as well as strongly enhanced influx of
399 MΦmono upon injection of MGO, a driver of PD-associated pathology [61]. However, in addition,
400 we demonstrated a drastic change in phenotype of MΦres. Importantly, this change in phenotype
401 translated into an enhanced response profile boosting pro-inflammatory effector molecule
402 production, which was maintained even when PD-fluid instillation was stopped. Thus, the
403 increased risk of developing pathological sequelae following repeated episodes of peritonitis in
404 PD patients is likely due to the damaging effect of the inflammatory response [66]. But our data
405 implies that patients on longterm PD treatment are at an increased risk to develop clinical
406 symptoms of peritonitis due to an enhanced inflammatory response of peritoneal resident cells.
407 Intriguingly, in PD patients receiving oral supplementation with vitamin D, a factor involved in the
408 expansion of peritoneal MΦres in mice [67], antibacterial responses were enhanced [68].
409 However, long-term consequences of this enhanced inflammation have not been investigated.

410
411 On the other hand, we have found enhanced expression of Arg-1, particularly in Physioneal
412 treated animals. Although, Arg-1 is typically considered a pro-fibrotic marker [69], expression of
413 Arg-1 specifically by macrophages has been shown to limit excessive ECM deposition in models of
414 liver fibrosis [70] and animals lacking Arg-1 expression specifically in myeloid cells fail to resolve
415 atherosclerotic inflammation and disease progression [71]. Taken together with the fact that
416 pathology-enhancing factors like peritonitis will lead to the disappearance of MΦres, as also
417 visible in our experiments using MGO, hints at a potential protective / anti-fibrotic role of MΦres,
418 as has previously been described in the kidney [39] and lung [72, 73]. Indeed, targeting
419 macrophages to induce an anti-fibrotic phenotype has previously been suggested [69]. Moreover,
420 recent single cell analysis of pro-resolving and pro-fibrotic macrophages following injury revealed
421 the presence of a unique macrophage population with enhanced phagocytosis and a gene
422 expression signature closely resembling resident macrophages [74, 75]. Thus, it may be feasible to
423 develop therapeutic approaches fostering a low-inflammatory, pro-resolving environment by
424 targeting and promoting homeostatic MΦres. Our data from *Salmonella enterica* ser.
425 Typhimurium infected mice indicated that the late stages of infection were linked to an increase
426 in Tim4 expressing MΦres as compared to naive animals. Similarly, previously published results
427 from helminth infected animals indicate enhanced expression of Tim4 on MΦres during the
428 chronic phase of these infection [76]. Hence, factors associated with the resolution of
429 inflammation or chronic Th2 immune responses may allow to 'rejuvenate' MΦres to regain some
430 of their homeostatic / anti-inflammatory activities. Further research is required to determine the
431 specific factors driving the MΦres phenotype as well as their potential use as therapeutic adjunct
432 during PD.

433
434 Independent of the therapeutic potential discussed above, analysing the immune cells contained
435 in the effluent of PD patients may yield a useful biomarker strategy. Changes in the composition
436 of myeloid cells as described by Liao et al. [12] as well as the assessment of cellular activation
437 markers, in particular their Interferon signature, as described in mice here, may allow risk-based

438 patient stratification. Patients likely to develop pathological sequelae of PD treatment could then
439 be prioritised for kidney transplant or transferred to haemodialysis prior to PD failure or before
440 overt pathology develops.

441

442 Lastly, our data comparing PBS injected animals to Physioneal injection indicated a limited
443 impact of the composition of the PD fluid on the observed physiological changes. In contrast, our
444 data using MGO as well as previously published reports have identified several constituents of PD
445 fluid, in particular lactate, GDP and low pH, to be instrumental in driving PD related pathology [77,
446 78]. However, while these factors have a clear impact on the inflammatory and pathological
447 response, our data is in line with a recent report investigating the use of so-called biocompatible
448 PD fluid in patients. Despite considerably lower levels of GDP and lactate in these solutions, the
449 morphological changes observed were very similar to those seen in patients utilising standard PD
450 fluid and even an early increase in microvascular density was detected [79]. Of note, it has been
451 suggested that this adverse effect of biocompatible PD fluid may be due to an altered
452 inflammatory response [80]. Thus, together with our data this suggests it may be more effective
453 to prevent pathological changes by targeting the elicited immune response to PD fluid
454 instillation, even in the absence of peritonitis. Due to this we also chose naive animals as
455 comparator, as these represent healthy patients not currently on PD, and hence the situation any
456 therapeutic intervention should aim to restore.

457

458 Taken together we have shown here that repeated exposure of the peritoneal microenvironment
459 to PD fluid instillation in mice led to a gradual change in phenotype as well as activation response
460 of peritoneal resident cells. These changes were relatively long lasting and resulted in a more
461 vigorous response to inflammatory triggers. Thus, targeting MΦres and preventing excessive
462 inflammatory responses in PD patients may pose an exciting novel approach to limit PD-related
463 pathology.

464

465 **Materials and Methods:**

466

467 **Ethics Statement**

468 All animal experiments were performed in accordance with the UK Animals (Scientific
469 Procedures) Act of 1986 under a Project License (70/8548) granted by the UK Home Office and
470 approved by the University of Manchester Ethical Review Committee.

471

471 **Mice and in vivo treatments**

472 Eight to 13 week old male and female C57BL/6 mice were obtained from a commercial vendor
473 (Envigo, Hillcrest, UK). Cx3cr1^{CreER} mice [58] were obtained from the Jackson Laboratory (Bar
474 Harbor, ME) bred in-house and crossed with R26R-EYFP animals (The Jackson Laboratory, Bar
475 Harbor, ME) [81] to generate Cx3cr1^{CreER}:R26-eyfp mice. All animals were maintained in groups of
476 4-6 animals in specific pathogen-free facilities at the University of Manchester. Experimental
477 mice were age and sex matched and randomly allocated to treatment groups using a computer-
478 based randomization technique and treatments were given following this a priori determined
479 order. Euthanasia was performed by asphyxiation in carbon dioxide in a rising concentration. No
480 experimental animals allocated to experimental groups were excluded from the analysis.
481 Researchers were not blinded to group allocations. Animal numbers were based on initial power
482 calculations of key determinants derived from preliminary experiments.
483 Animals were injected i.p. with 500 µL peritoneal dialysis fluid (Physioneal 40, 3.86% glucose,
484 Baxter HealthCare Ltd., Compton, UK) for the indicated number of injections supplemented with
485 40 mM Methylglyoxal (Sigma Adlrich) where indicated. Injections were carried out daily or every
486 other day for three or five days per week for up to 4 weeks (maximum 14 injections per animal).

487 Control animals were left untreated or received an equal volume of PBS i.p. as indicated.
488 For the induction of inflammatory responses PD fluid treated mice received intra-peritoneal
489 injections of 400 μ L 4% Brewer modified thioglycollate medium (BD Biosciences, San Jose, CA) or
490 sterile saline as control. The attenuated *Salmonella enterica* serovar Typhimurium strain SL3261
491 (Δ aroA) [82] was cultured overnight at 37°C in a shaking incubator from frozen stock in Luria-
492 Bertani broth with 50 μ g/mL streptomycin. The following morning, culture was diluted in fresh
493 Luria-Bertani broth with 50 μ g/mL streptomycin and incubated at 37°C in a shaking incubator to
494 ensure the bacteria were in the growth phase. CFU/mL was estimated by the OD600 reading.
495 Animals were pre-treated with 20 mg streptomycin 1 day prior to oral infection with $\sim 1 \times 10^8$ CFU
496 *Salmonella* Typhimurium diluted in PBS. Infectious doses and peritoneal bacterial burdens were
497 enumerated by plating inocula or peritoneal exudate cells in 10-fold serial dilutions in PBS on LB-
498 Agar plates.

499 Cell-isolation

500 Peritoneal cavity exudate cells (PEC) were obtained by washing the cavity with 10 mL lavage
501 media comprised of RPMI 1640 (Sigma-Aldrich, Dorset, UK) containing 2 mM EDTA and 1% L-
502 Glutamine (Thermo Fisher Scientific, Waltham, MA). Erythrocytes were removed by incubating
503 with red blood cell lysis buffer (Sigma-Aldrich). Cellular content was assessed by cell counting
504 using Viastain AO/PI solution on a Cellometer[®] Auto 2000 Cell Counter (Nexcelom Bioscience,
505 Manchester, UK) in combination with multicolor flow cytometry.

506 Flow cytometry

507 Equal numbers of cells were stained with Zombie UV viability assay (Biolegend, London, UK). All
508 samples were then blocked with 5 μ g/mL anti CD16/32 (93; BioLegend Cat# 101301,
509 RRID:AB_312800) and heat-inactivated normal mouse serum (1:10, Sigma-Aldrich) in flow
510 cytometry buffer (0.5% BSA and 2 mM EDTA in Dulbecco's PBS) before surface staining on ice
511 with antibodies to F4/80 (BM8; Cat# 123146, RRID:AB_2564133), SiglecF (E502440, BD
512 Biosciences Cat# 562681, RRID:AB_2722581), Ly6C (HK1.4; Cat# 128033, RRID:AB_2562351), Ly-
513 6G (1A8; Cat# 127612, RRID:AB_2251161), TCR β (H57-597; Cat# 109226, RRID:AB_1027649),
514 CD11b (M1/70; Cat# 101242, RRID:AB_2563310), CD11c (N418; Cat# 117334, RRID:AB_2562415),
515 I-A/I-E (M5/114.15.2; Cat# 107622, RRID:AB_493727), CD19 (6D5; Cat# 115523, RRID:AB_439718),
516 CD115 (AFS98; Cat# 135530, RRID:AB_2566525), CD73 (TY/11.8; Cat# 127206,
517 RRID:AB_2154094), CD102 (3C4 (MIC2/4); Cat# 105604, RRID:AB_313197), Tim4 (RMT4-54; Cat#
518 130010, RRID:AB_2565719), CD206 (MR6F3; Cat# 141723, RRID:AB_2562445), Vsig4 (NLA14;
519 Thermo Fisher Scientific Cat# 17-5752-82, RRID:AB_2637429), CD226 (10E5; Cat# 128816,
520 RRID:AB_2632821), Sca1/Ly6A (D7; Cat# 108139, RRID:AB_2565957). All antibodies were
521 purchased from Biolegend unless stated otherwise.

522 Detection of intracellular activation markers was performed directly ex vivo. Cells were stained
523 for surface markers then fixed and permeabilized for at least 16 h using the eBioscience™ Foxp3/
524 Transcription Factor Staining Buffer Set (Thermo Fisher Scientific). Cells were then stained with
525 directly labeled Abs to NOS2 (CXNFT; Thermo Fisher Scientific Cat# 25-5920-82,
526 RRID:AB_2573499), Arg1 (polyclonal, R and D Systems Cat# IC5868A, RRID:AB_2810265), Ki67
527 (B56, BD Biosciences Cat# 563755, RRID:AB_2738406), Annexin V (Biolegend), Gata-6 (D61E4;
528 Cell Signaling Technology Cat# 26452, RRID:AB_2798924) or purified polyclonal rabbit anti-
529 Rel α (PeproTech Cat# 500-P214-50ug, RRID:AB_1268843) and biotinylated anti-Ym1/2
530 (polyclonal, R and D Systems Cat# BAF2446, RRID:AB_2260451) followed by Zenon anti-rabbit
531 reagent (Thermo Fisher Scientific Cat# Z25302, RRID:AB_2572214) or streptavidin BUV 737 (BD
532 Biosciences Cat# 612775, RRID:AB_2870104), respectively.

533 Samples were acquired on a BD LSR II or BD FACSymphony using BD FACSDiva software (BD
534 Biosciences) and post-acquisition analysis performed using FlowJo v10 software (BD Biosciences).

535 Cell-culture experiments

536 For in vitro stimulation of PD fluid-conditioned cells, whole PEC were counted as described above
537 and seeded to 96-well U bottom plates at 3×10^5 cells per well in RPMI 1640 containing 5 % foetal
538 bovine serum, 2 mM L-glutamine, 100 U/mL penicillin and 100 µg/mL streptomycin and
539 stimulated with lipopolysaccharide (LPS, 100 ng/mL; *Salmonella enterica* ser. Typhimurium;
540 Sigma-Aldrich) and recombinant murine Interferon γ (IFN γ , 20 ng/mL PeproTech EC Ltd.) or
541 medium alone for 6 h or with murine recombinant Interleukin-4 (rIL-4, 20 ng/mL, PeproTech EC
542 Ltd.) for 24 h and analysed for M Φ activation markers by flow cytometry.

543 **Apoptotic cell uptake assay**

544 Uptake of apoptotic cells by peritoneal M Φ res was assessed as previously described (52). Briefly,
545 thymocytes were collected from naive animals by mincing thymi through 2 µm gauze until
546 completely homogenized. Erythrocytes were removed by incubating with red blood cell lysis
547 buffer (Sigma-Aldrich). Thymocytes were resuspended at 1×10^7 cells/mL in complete DMEM and
548 incubated in the presence of 0.1 µM dexamethasone (Sigma-Aldrich) at 37 °C for 18 h. This
549 produced >90 % apoptosis, as assessed by Viastain AO/PI staining measured on a Cellometer ®
550 Auto 2000 Cell Counter (Nexcelom Bioscience). Subsequently, apoptotic thymocytes were
551 washed twice with PBS and resuspended in PBS at 10^6 cells/mL containing 40 ng/mL pHrodo-
552 SE (Thermo Fisher Scientific) and incubated at RT for 30 min. Thereafter the cells were washed
553 twice with PBS and resuspended in RPMI containing 5 % foetal bovine serum, 2 mM L-glutamine,
554 100 U/mL penicillin and 100 µg/mL streptomycin. Unstained apoptotic cells served as staining
555 control.

556 **RNA-isolation and NanoString analysis**

557 Whole PEC were isolated as described above and total RNA isolated using Tri-reagent (Thermo
558 Fisher Scientific) as described by the manufacturer. RNA concentration was determined using the
559 Qbit and RNA-BR kit (Thermo Fisher Scientific). Samples were diluted and 100 ng of RNA was
560 processed for running on a NanoString nCounter FLEX system using the nCounter Mouse Fibrosis
561 V2 panel (NanoString Technologies Inc., Seattle, WA). Raw counts were normalized to internal
562 spike-in controls and the expression of 10 stable housekeeping genes using the geNorm
563 algorithm and differential gene expression calculated using the nSolver Analysis software 4.0
564 Advanced Analysis tool (NanoString Technologies). The datasets for this study can be found in
565 Figshare available under DOI:10.48420/14635917.

566 **Statistical analysis**

567 Statistical analysis was performed using Prism 8 for Mac OS X (v8.2.1, GraphPad Prism,
568 RRID:SCR_002798). Differences between groups were determined by t-test or ANOVA followed
569 by Tukey's or Dunn's multiple comparison-test. In some cases data was log-transformed to
570 achieve normal distribution as determined by optical examination of residuals. Where this was
571 not possible a Mann-Whitney or Kruskal-Wallis test was used. Percentages were subjected to
572 arcsine transformation prior to analysis. Differences were assumed statistically significant for *P*
573 values of less than 0.05.

574

575 **Author contributions**

- 576 - TES: Resources, Writing – Review & Editing, Funding Acquisition
- 577 - TNS: Investigation, Resources, Writing – Review & Editing
- 578 - RL: Resources, Writing – Review and Editing, Clinical advice
- 579 - SEH: Conceptualization, Writing – Review and Editing
- 580 - DR: Conceptualization, Formal Analysis, Validation, Investigation, Writing - Original Draft
- 581 Preparation, Writing – Review and Editing, Visualization, Project Administration, Funding
- 582 Acquisition
- 583

584 **Competing interests**

585 The authors declare that they have no competing interests.

586

587 **List of abbreviations**

588 GDP: glucose degradation products

589 MΦ: macrophage

590 MΦres: tissue resident macrophage

591 MΦmono: monocyte-derived macrophage

592 MGO: Methylglyoxal

593 PEC: peritoneal exudate cells

594 PD: peritoneal dialysis

595 HD: Haemodialysis

596

597 **Acknowledgements**

598 This work was supported by the Medical Research Council UK (MR/P02615X/1, DR) and the
599 Medical Research Foundation / Asthma UK (MRFAUK-2015-302, TES). TNS was supported by
600 a BBSRC Discovery Research Fellowship (BB/S01103X/1, TNS), RL was supported by a Wellcome
601 Trust Senior Fellowship award (202860/Z/16/Z, RL) and SEH and DR were supported by an MRC
602 Research Grant (MRC MR/S02560X/1, SEH). The nCounter transcript analysis was supported by a
603 University of Manchester Immunology Gene Expression Panel Grant (NanoString Technologies
604 Inc., Seattle, WA).

605 We thank Dr. Gareth Howell from the Flow Cytometry Core Facility at the University of
606 Manchester for assistance with the flow cytometry analyses. We'd also like to thank Sister Trish
607 Smith from the Royal Manchester Children's Hospital for the provision of Physioneal 40, Dr John
608 Grainger (University of Manchester, UK) for the provision of the Cx3cr1^{CreER}:R26-eyfp mice as well
609 as Prof. Judith E. Allen (University of Manchester, UK) for use of her Home Office animal licence
610 and critical appraisal of the work.

611

612 **References:**

613

- 614 1. Luyckx, V.A., M. Tonelli, and J.W. Stanifer, The global burden of kidney disease and the
615 sustainable development goals. *Bull World Health Organ*, 2018. **96**(6): p. 414-422D.
- 616 2. Kramer, A., et al., The European Renal Association - European Dialysis and Transplant
617 Association (ERA-EDTA) Registry Annual Report 2016: a summary. *Clin Kidney J*, 2019. **12**(5):
618 p. 702-720.
- 619 3. van de Luijngaarden, M.W., et al., Trends in dialysis modality choice and related patient
620 survival in the ERA-EDTA Registry over a 20-year period. *Nephrol Dial Transplant*, 2016. **31**(1):
621 p. 120-8.
- 622 4. Chui, B.K., et al., Health care costs of peritoneal dialysis technique failure and dialysis
623 modality switching. *Am J Kidney Dis*, 2013. **61**(1): p. 104-11.
- 624 5. Francois, K. and J.M. Bargman, Evaluating the benefits of home-based peritoneal dialysis.
625 *Int J Nephrol Renovasc Dis*, 2014. **7**: p. 447-55.
- 626 6. Bartosova, M. and C.P. Schmitt, Biocompatible Peritoneal Dialysis: The Target Is Still Way
627 Off. *Front Physiol*, 2018. **9**: p. 1853.
- 628 7. Morelle, J., et al., Interstitial Fibrosis Restricts Osmotic Water Transport in Encapsulating
629 Peritoneal Sclerosis. *J Am Soc Nephrol*, 2015. **26**(10): p. 2521-33.
- 630 8. Johnson, D.W., et al., Encapsulating peritoneal sclerosis: incidence, predictors, and
631 outcomes. *Kidney Int*, 2010. **77**(10): p. 904-12.
- 632 9. Moinuddin, Z., et al., Encapsulating peritoneal sclerosis-a rare but devastating peritoneal
633 disease. *Front Physiol*, 2014. **5**: p. 470.

- 634 10. Danford, C.J., et al., Encapsulating peritoneal sclerosis. *World J Gastroenterol*, 2018.
635 **24**(28): p. 3101-3111.
- 636 11. Wang, J., et al., The role of peritoneal alternatively activated macrophages in the process of
637 peritoneal fibrosis related to peritoneal dialysis. *Int J Mol Sci*, 2013. **14**(5): p. 10369-82.
- 638 12. Liao, C.T., et al., Peritoneal macrophage heterogeneity is associated with different
639 peritoneal dialysis outcomes. *Kidney Int*, 2017. **91**(5): p. 1088-1103.
- 640 13. Minutti, C.M., et al., Local amplifiers of IL-4Ralpha-mediated macrophage activation
641 promote repair in lung and liver. *Science*, 2017. **356**(6342): p. 1076-1080.
- 642 14. Li, Q., et al., A pathogenetic role for M1 macrophages in peritoneal dialysis-associated
643 fibrosis. *Mol Immunol*, 2018. **94**: p. 131-139.
- 644 15. Gordon, S. and A. Pluddemann, Tissue macrophages: heterogeneity and functions. *BMC*
645 *Biol*, 2017. **15**(1): p. 53.
- 646 16. Zhao, Y., et al., The origins and homeostasis of monocytes and tissue-resident macrophages
647 in physiological situation. *J Cell Physiol*, 2018. **233**(10): p. 6425-6439.
- 648 17. Gundra, U.M., et al., Alternatively activated macrophages derived from monocytes and
649 tissue macrophages are phenotypically and functionally distinct. *Blood*, 2014. **123**(20): p. e110-22.
- 650 18. Ruckerl, D., et al., Macrophage origin limits functional plasticity in helminth-bacterial co-
651 infection. *PLoS Pathog*, 2017. **13**(3): p. e1006233.
- 652 19. Uderhardt, S., et al., 12/15-lipoxygenase orchestrates the clearance of apoptotic cells and
653 maintains immunologic tolerance. *Immunity*, 2012. **36**(5): p. 834-46.
- 654 20. Allen, J.E. and D. Ruckerl, The Silent Undertakers: Macrophages Programmed for
655 Efferocytosis. *Immunity*, 2017. **47**(5): p. 810-812.
- 656 21. Wang, J. and P. Kubes, A Reservoir of Mature Cavity Macrophages that Can Rapidly
657 Invade Visceral Organs to Affect Tissue Repair. *Cell*, 2016. **165**(3): p. 668-78.
- 658 22. Barth, M.W., et al., Review of the macrophage disappearance reaction. *J Leukoc Biol*, 1995.
659 **57**(3): p. 361-7.
- 660 23. Accarias, S., et al., Single-cell analysis reveals new subset markers of murine peritoneal
661 macrophages and highlights macrophage dynamics upon *Staphylococcus aureus* peritonitis. *Innate*
662 *Immun*, 2016. **22**(5): p. 382-92.
- 663 24. Jonjic, N., et al., Expression of adhesion molecules and chemotactic cytokines in cultured
664 human mesothelial cells. *J Exp Med*, 1992. **176**(4): p. 1165-74.
- 665 25. Zhang, N., et al., Expression of factor V by resident macrophages boosts host defense in the
666 peritoneal cavity. *J Exp Med*, 2019. **216**(6): p. 1291-1300.
- 667 26. Davies, L.C., et al., Distinct bone marrow-derived and tissue-resident macrophage lineages
668 proliferate at key stages during inflammation. *Nat Commun*, 2013. **4**: p. 1886.
- 669 27. Misharin, A.V., et al., Monocyte-derived alveolar macrophages drive lung fibrosis and
670 persist in the lung over the life span. *J Exp Med*, 2017. **214**(8): p. 2387-2404.
- 671 28. Braga, T.T., et al., CCR2 contributes to the recruitment of monocytes and leads to kidney
672 inflammation and fibrosis development. *Inflammopharmacology*, 2018. **26**(2): p. 403-411.
- 673 29. Puranik, A.S., et al., Kidney-resident macrophages promote a proangiogenic environment in
674 the normal and chronically ischemic mouse kidney. *Sci Rep*, 2018. **8**(1): p. 13948.
- 675 30. Lee, S.H., et al., The monocyte chemoattractant protein-1 (MCP-1)/CCR2 system is
676 involved in peritoneal dialysis-related epithelial-mesenchymal transition of peritoneal mesothelial
677 cells. *Lab Invest*, 2012. **92**(12): p. 1698-711.
- 678 31. Chen, Y.T., et al., Inflammatory macrophages switch to CCL17-expressing phenotype and
679 promote peritoneal fibrosis. *J Pathol*, 2020. **250**(1): p. 55-66.
- 680 32. Lambie, M.R., et al., Peritoneal inflammation precedes encapsulating peritoneal sclerosis:
681 results from the GLOBAL Fluid Study. *Nephrol Dial Transplant*, 2016. **31**(3): p. 480-6.
- 682 33. Moriishi, M., et al., Preservation of peritoneal catheter for prevention of encapsulating
683 peritoneal sclerosis. *Adv Perit Dial*, 2002. **18**: p. 149-53.
- 684 34. Bellon, T., et al., Alternative activation of macrophages in human peritoneum: implications
685 for peritoneal fibrosis. *Nephrol Dial Transplant*, 2011. **26**(9): p. 2995-3005.

- 686 35. Chandrasekaran, P., et al., Regulatory Macrophages Inhibit Alternative Macrophage
687 Activation and Attenuate Pathology Associated with Fibrosis. *J Immunol*, 2019. **203**(8): p. 2130-
688 2140.
- 689 36. Han, Y., et al., Role of macrophages in the fibrotic phase of rat crescentic
690 glomerulonephritis. *Am J Physiol Renal Physiol*, 2013. **304**(8): p. F1043-53.
- 691 37. Nikolic-Paterson, D.J., S. Wang, and H.Y. Lan, Macrophages promote renal fibrosis through
692 direct and indirect mechanisms. *Kidney Int Suppl* (2011), 2014. **4**(1): p. 34-38.
- 693 38. Wang, Y., et al., Ex vivo programmed macrophages ameliorate experimental chronic
694 inflammatory renal disease. *Kidney Int*, 2007. **72**(3): p. 290-9.
- 695 39. Ferenbach, D.A., et al., Macrophage/monocyte depletion by clodronate, but not diphtheria
696 toxin, improves renal ischemia/reperfusion injury in mice. *Kidney Int*, 2012. **82**(8): p. 928-33.
- 697 40. Boulanger, E., et al., Mesothelial RAGE activation by AGEs enhances VEGF release and
698 potentiates capillary tube formation. *Kidney Int*, 2007. **71**(2): p. 126-33.
- 699 41. Davies, L.C., et al., A quantifiable proliferative burst of tissue macrophages restores
700 homeostatic macrophage populations after acute inflammation. *Eur J Immunol*, 2011. **41**(8): p.
701 2155-64.
- 702 42. Miyanishi, M., et al., Identification of Tim4 as a phosphatidylserine receptor. *Nature*, 2007.
703 **450**(7168): p. 435-9.
- 704 43. Miyanishi, M., K. Segawa, and S. Nagata, Synergistic effect of Tim4 and MFG-E8 null
705 mutations on the development of autoimmunity. *Int Immunol*, 2012. **24**(9): p. 551-9.
- 706 44. Li, J., et al., VSIG4 inhibits proinflammatory macrophage activation by reprogramming
707 mitochondrial pyruvate metabolism. *Nat Commun*, 2017. **8**(1): p. 1322.
- 708 45. Yuan, X., et al., CR1g, a tissue-resident macrophage specific immune checkpoint molecule,
709 promotes immunological tolerance in NOD mice, via a dual role in effector and regulatory T cells.
710 *Elife*, 2017. **6**.
- 711 46. Heng, T.S., M.W. Painter, and C. Immunological Genome Project, The Immunological
712 Genome Project: networks of gene expression in immune cells. *Nat Immunol*, 2008. **9**(10): p. 1091-
713 4.
- 714 47. Hasko, G., et al., Ecto-5'-nucleotidase (CD73) decreases mortality and organ injury in
715 sepsis. *J Immunol*, 2011. **187**(8): p. 4256-67.
- 716 48. Rosas, M., et al., The transcription factor Gata6 links tissue macrophage phenotype and
717 proliferative renewal. *Science*, 2014. **344**(6184): p. 645-648.
- 718 49. Okabe, Y. and R. Medzhitov, Tissue-specific signals control reversible program of
719 localization and functional polarization of macrophages. *Cell*, 2014. **157**(4): p. 832-44.
- 720 50. Kitterer, D., et al., Gender-Specific Differences in Peritoneal Dialysis. *Kidney Blood Press*
721 *Res*, 2017. **42**(2): p. 276-283.
- 722 51. Bain, C.C., et al., Long-lived self-renewing bone marrow-derived macrophages displace
723 embryo-derived cells to inhabit adult serous cavities. *Nat Commun*, 2016. **7**: p. ncomms11852.
- 724 52. Lopez-Castejon, G., A. Baroja-Mazo, and P. Pelegrin, Novel macrophage polarization
725 model: from gene expression to identification of new anti-inflammatory molecules. *Cell Mol Life*
726 *Sci*, 2011. **68**(18): p. 3095-107.
- 727 53. Miksa, M., et al., A novel method to determine the engulfment of apoptotic cells by
728 macrophages using pHrodo succinimidyl ester. *J Immunol Methods*, 2009. **342**(1-2): p. 71-7.
- 729 54. Gautier, E.L., et al., Local apoptosis mediates clearance of macrophages from resolving
730 inflammation in mice. *Blood*, 2013. **122**(15): p. 2714-22.
- 731 55. Menzies, F.M., et al., Sequential expression of macrophage anti-microbial/inflammatory and
732 wound healing markers following innate, alternative and classical activation. *Clin Exp Immunol*,
733 2010. **160**(3): p. 369-79.
- 734 56. Zhang, S., et al., Delineation of diverse macrophage activation programs in response to
735 intracellular parasites and cytokines. *PLoS Negl Trop Dis*, 2010. **4**(3): p. e648.
- 736 57. Ruckerl, D. and P.C. Cook, Macrophages assemble! But do they need IL-4R during
737 schistosomiasis? *Eur J Immunol*, 2019. **49**(7): p. 996-1000.

- 738 58. Yona, S., et al., Fate mapping reveals origins and dynamics of monocytes and tissue
739 macrophages under homeostasis. *Immunity*, 2013. **38**(1): p. 79-91.
- 740 59. Bain, C.C. and S.J. Jenkins, The biology of serous cavity macrophages. *Cell Immunol*,
741 2018. **330**: p. 126-135.
- 742 60. Wieslander, A., et al., Cytotoxicity, pH, and glucose degradation products in four different
743 brands of PD fluid. *Adv Perit Dial*, 1996. **12**: p. 57-60.
- 744 61. Kitamura, M., et al., Epigallocatechin gallate suppresses peritoneal fibrosis in mice. *Chem*
745 *Biol Interact*, 2012. **195**(1): p. 95-104.
- 746 62. Sica, A., et al., Macrophage polarization in pathology. *Cell Mol Life Sci*, 2015. **72**(21): p.
747 4111-26.
- 748 63. Ribatti, D., Mast cells and macrophages exert beneficial and detrimental effects on tumor
749 progression and angiogenesis. *Immunol Lett*, 2013. **152**(2): p. 83-8.
- 750 64. Wynn, T.A. and K.M. Vannella, Macrophages in Tissue Repair, Regeneration, and Fibrosis.
751 *Immunity*, 2016. **44**(3): p. 450-462.
- 752 65. Guillot, A. and F. Tacke, Liver Macrophages: Old Dogmas and New Insights. *Hepatology*
753 *Commun*, 2019. **3**(6): p. 730-743.
- 754 66. Williams, J.D., et al., Morphologic changes in the peritoneal membrane of patients with
755 renal disease. *J Am Soc Nephrol*, 2002. **13**(2): p. 470-9.
- 756 67. Song, L., et al., The Vitamin D Receptor Regulates Tissue Resident Macrophage Response
757 to Injury. *Endocrinology*, 2016. **157**(10): p. 4066-4075.
- 758 68. Bacchetta, J., et al., Antibacterial responses by peritoneal macrophages are enhanced
759 following vitamin D supplementation. *PLoS One*, 2014. **9**(12): p. e116530.
- 760 69. Adhyatmika, A., et al., The Elusive Antifibrotic Macrophage. *Front Med (Lausanne)*, 2015.
761 **2**: p. 81.
- 762 70. Pesce, J.T., et al., Arginase-1-expressing macrophages suppress Th2 cytokine-driven
763 inflammation and fibrosis. *PLoS Pathog*, 2009. **5**(4): p. e1000371.
- 764 71. Yurdagul, A., Jr., et al., Macrophage Metabolism of Apoptotic Cell-Derived Arginine
765 Promotes Continual Efferocytosis and Resolution of Injury. *Cell Metab*, 2020. **31**(3): p. 518-533
766 e10.
- 767 72. Khalil, N., et al., Plasmin regulates the activation of cell-associated latent TGF-beta 1
768 secreted by rat alveolar macrophages after in vivo bleomycin injury. *Am J Respir Cell Mol Biol*,
769 1996. **15**(2): p. 252-9.
- 770 73. Reddy, A.T., et al., Nitrated fatty acids reverse pulmonary fibrosis by dedifferentiating
771 myofibroblasts and promoting collagen uptake by alveolar macrophages. *FASEB J*, 2014. **28**(12): p.
772 5299-310.
- 773 74. Perciani, C.T. and S.A. MacParland, Lifting the veil on macrophage diversity in tissue
774 regeneration and fibrosis. *Sci Immunol*, 2019. **4**(40).
- 775 75. Sommerfeld, S.D., et al., Interleukin-36gamma-producing macrophages drive IL-17-
776 mediated fibrosis. *Sci Immunol*, 2019. **4**(40).
- 777 76. Campbell, S.M., et al., Myeloid cell recruitment versus local proliferation differentiates
778 susceptibility from resistance to filarial infection. *Elife*, 2018. **7**.
- 779 77. Krishnan, M., et al., Glucose degradation products (GDP's) and peritoneal changes in
780 patients on chronic peritoneal dialysis: will new dialysis solutions prevent these changes? *Int Urol*
781 *Nephrol*, 2005. **37**(2): p. 409-18.
- 782 78. Mortier, S., et al., Benefits of switching from a conventional to a low-GDP
783 bicarbonate/lactate-buffered dialysis solution in a rat model. *Kidney Int*, 2005. **67**(4): p. 1559-65.
- 784 79. Schaefer, B., et al., Neutral pH and low-glucose degradation product dialysis fluids induce
785 major early alterations of the peritoneal membrane in children on peritoneal dialysis. *Kidney Int*,
786 2018. **94**(2): p. 419-429.
- 787 80. Blake, P.G., Is the peritoneal dialysis biocompatibility hypothesis dead? *Kidney Int*, 2018.
788 **94**(2): p. 246-248.

- 789 81. Srinivas, S., et al., Cre reporter strains produced by targeted insertion of EYFP and ECFP
790 into the ROSA26 locus. *BMC Dev Biol*, 2001. **1**: p. 4.
791 82. Hoiseth, S.K. and B.A. Stocker, Aromatic-dependent *Salmonella typhimurium* are non-
792 virulent and effective as live vaccines. *Nature*, 1981. **291**(5812): p. 238-9.

793
794

795 **Figure legends:**

796

797 **Figure 1: Injection of dialysis fluid alters peritoneal myeloid cell composition**

798 C57BL/6 mice were injected with Physioneal (filled circles) or left untreated (open squares) and whole PEC isolated 6
799 h later. Cells were counted and analysed by flow cytometry to determine the number of A) MΦres (lineage-CD11b+,
800 F₄/80high, MHC-II low), B) neutrophils (lineage +, SSC mid, MHC-II-, F₄/80-, CD11b+), C) monocytes (lineage-CD11b+,
801 F₄/80-, MHC-II low, Ly6C high) and D) MΦ_{mono} (lineage-CD11b+, F₄/80low, MHC-II high). E) Histogram and
802 quantitative data of fluorescence mean intensity of MHC-II expression by MΦ_{mono} (grey, dashed line) or MΦres
803 from Physioneal injected (black, solid line) or naive animals (grey, solid line). F-H) Expression of CD206, Ym1 and
804 binding of Annexin V by MΦres identified in A) assessed by flow cytometry. Datapoints depict individual animals and
805 bars indicate mean and SD. Data pooled from 4 independent experiments using 3-5 animals per group. Data analysed
806 using a Mann-Whitney-U test after transformation. n.s.: not significant; *: p<0.05; **: p<0.01; ****: p<0.0001
807 lineage: TCRβ CD19 Siglec-F Ly6G
808

809 **Figure 2: Repeated injection of PD fluid leads to a progressive change in MPres phenotype**

810 C57BL/6 mice were injected with PD fluid (filled circle) or left untreated (open square) 5 times a week for the
811 indicated number of injections. At each timepoint whole PEC were isolated 24 h after the last injection and analysed
812 by flow cytometry. A) Schematic depiction of experimental timeline. B-D) Number of MΦres, MΦ_{mono} and Ly6C
813 high monocytes. E-H) Expression of MΦres associated cell-surface markers on F₄/80 high MΦ. I) Intracellular
814 expression of Gata6 in MΦres identified in A).
815 Datapoints depict individual animals and lines indicate (B-H) median or (I) mean with SD. Data from a single
816 experiment using 3 animals per group per timepoint. Data analysed using 2-way ANOVA followed by Tukey's post-
817 hoc test after transformation. n.s.: not significant; *: p<0.05; **: p<0.01; ****: p<0.0001
818

819 **Figure 3: Chronic inflammation induced by *S.Typhimurium* infection does not phenocopy repeated PD fluid
820 injection**

821 C57BL/6 mice were infected orally with 1x10⁸ cfu *S.Typhimurium* (closed rhombus) or left untreated (open squares)
822 and peritoneal cells analysed 34 (d₃₄) and 55 days (d₅₅) post infection. Dotplot (d₅₅) and quantification of MHC-II (A)
823 and Sca-1 (B) expression by MΦres assessed by flow cytometry C) Number of peritoneal neutrophils. D) Enumeration
824 of bacterial colony forming units present in the peritoneal cavity. E-G) Expression of MΦres associated cell surface
825 markers assessed by flow cytometry.
826 Datapoints depict individual animals and bars / lines indicate mean with SD. Data representative of one (d₃₄) or two
827 (d₅₅) separate experiments using 3-4 animals per group per timepoint. Data analysed using 2-way ANOVA followed
828 by Tukey's post-hoc test after transformation. n.s.: not significant; *: p<0.05; **: p<0.01; ****: p<0.001
829

830 **Figure 4: Repeated injection of sterile saline induces similar alterations to dialysis fluid**

831 A) Female C57BL/6 mice were injected 5 times a week for a total of nine injections with Physioneal (circles), sterile
832 PBS (triangles) or left untreated (squares). 24 h after the last injection whole PEC were isolated and analysed by flow
833 cytometry for expression of MΦres associated cell-surface markers. Data pooled from two independent experiments.
834 B) Male (♂) and female (♀) C57BL/6 mice were injected 5 times a week for a total of nine injections with PD fluid
835 (dark symbols) or left untreated (light symbols). 24 h after the last injection whole PEC were isolated and analysed as
836 described for A).
837 Datapoints depict individual animals and lines indicate mean and SD. Data from a single experiment.
838 Data analysed using 2-way ANOVA followed by Tukey's multiple comparison test after transformation. n.s.: not
839 significant; *: p<0.05; **: p<0.01; ****: p<0.0001
840

841 **Figure 5: MΦres from PD fluid-injected animals show progressively enhanced responses to stimulation**

842 C57BL/6 mice were injected with PD fluid (circles) or left untreated (squares) 5 times a week for the indicated number
843 of injections. At each timepoint whole PEC were isolated 24 h after the last injection and incubated in vitro in the

844 presence of pHrodo labelled apoptotic thymocytes for 90 minutes (A & B) or stimulated with LPS/IFN γ (C & D; 6 h) or
845 recombinant IL-4 (E & F; 24 h).
846 Uptake of apoptotic cells by total CD11b⁺ myeloid cells (A) or M Φ res (CD102+I-A/I-E low) (B) as well as expression of
847 M Φ res associated cell-surface markers (C-F) assessed by flow cytometry.
848 Datapoints depict individual animals and lines indicate mean and SD. Data from a single experiment. Data analysed
849 using 2-way ANOVA followed by Tukey's post-hoc test after transformation. n.s.: not significant; *: p<0.05; **:
850 p<0.01; ****: p<0.0001
851

852 **Figure 6: PD fluid conditioned M Φ res maintain altered activation phenotype after treatment is discontinued**
853 **while remaining largely tissue-resident derived.**
854 (A) C57BL/6 mice were injected 5 times a week for a total of nine injections with Physioneal (circles), sterile PBS
855 (triangles) or left untreated (squares). 7 days after the last injection whole PEC were isolated and analysed by flow
856 cytometry for expression of M Φ res associated cell-surface markers. (B) The cells isolated in (A) were subjected to in
857 vitro stimulation with LPS/IFN γ (6 h) and analysed by flow cytometry for NOS2 & Sca1 expression. C&D) To
858 determine the cellular origin of the M Φ res Cx3cr1^{CreER}:R26-eyfp mice were treated as described in (A) and additionally
859 received 5 doses of tamoxifen per oral gavage at the beginning of the experiment. (C) Schematic depiction of the
860 experimental timeline for experiments with tamoxifen injection. (D) Analysis of eYFP expression by M Φ res and
861 M Φ mono in Cx3cr1^{CreER}:R26-eyfp mice treated with PBS, Physioneal or untreated.
862 Datapoints depict individual animals and lines indicate mean & SD. (A, B) Data pooled from 2 independent
863 experiments. Data analysed using 2-way ANOVA followed by Tukey's multiple comparison test after transformation.
864 (D) Data from 2 independent experiments analysed by 2-way ANOVA followed by Tukey's multiple comparison test
865 after transformation. # indicate statistical differences between M Φ res and M Φ mono of the same treatment.
866 n.s.: not significant; *: p<0.05; **: p<0.01; ***: p<0.001; ****: p<0.0001;
867

868 **Figure 7: Addition of glucose-degradation products strongly enhances peritoneal inflammation.** C57BL/6 mice
869 were injected with PD fluid (Phys, circles) or PD fluid supplemented with 40 mM Methylglyoxal (MGO, triangles) or
870 were left untreated (naive, squares) 5 times a week for a total of 14 injections and analysed 24 h after the last
871 injection. (A) Number of inflammatory cells isolated from the peritoneal cavity. (B) Sample dot plots depicting
872 myeloid cells (CD11b⁺, lineage -) isolated from the animals in (A). (C & D) Expression of M Φ res associated surface
873 markers (C) as well as M Φ activation markers (D). Datapoints depict individual animals and bars indicate mean and
874 SD. Data from 3 independent experiments. Data analysed using 2-way ANOVA followed by Tukey's post-hoc test
875 after transformation. n.s.: not significant; *: p<0.05; **: p<0.01; ***: p<0.001; ****: p<0.0001
876 (E-G) nCounter fibrosis panel analysis of whole PEC isolated in (A). Bars indicate genes upregulated in naive (purple),
877 Physioneal (orange) or Physioneal + Methylglyoxal (blue) treated animals. Data depicted as log₂ fold change of
878 significantly differentially expressed genes (p<0.05) as mean and SEM of three animals per group.
879

Figure 1

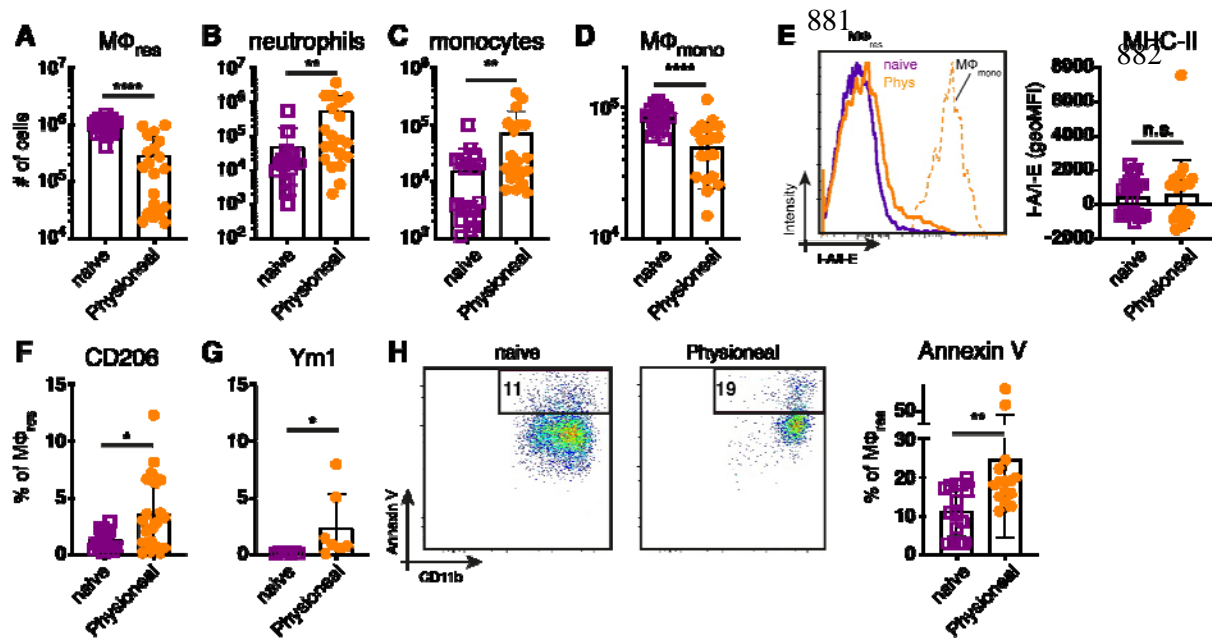


Figure 2

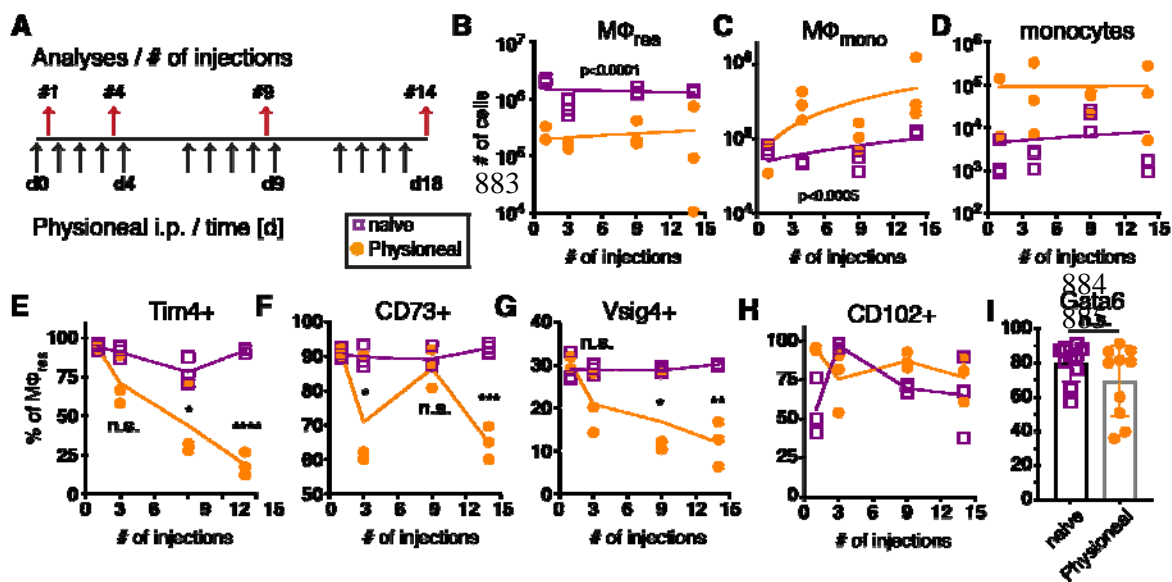


Figure 3

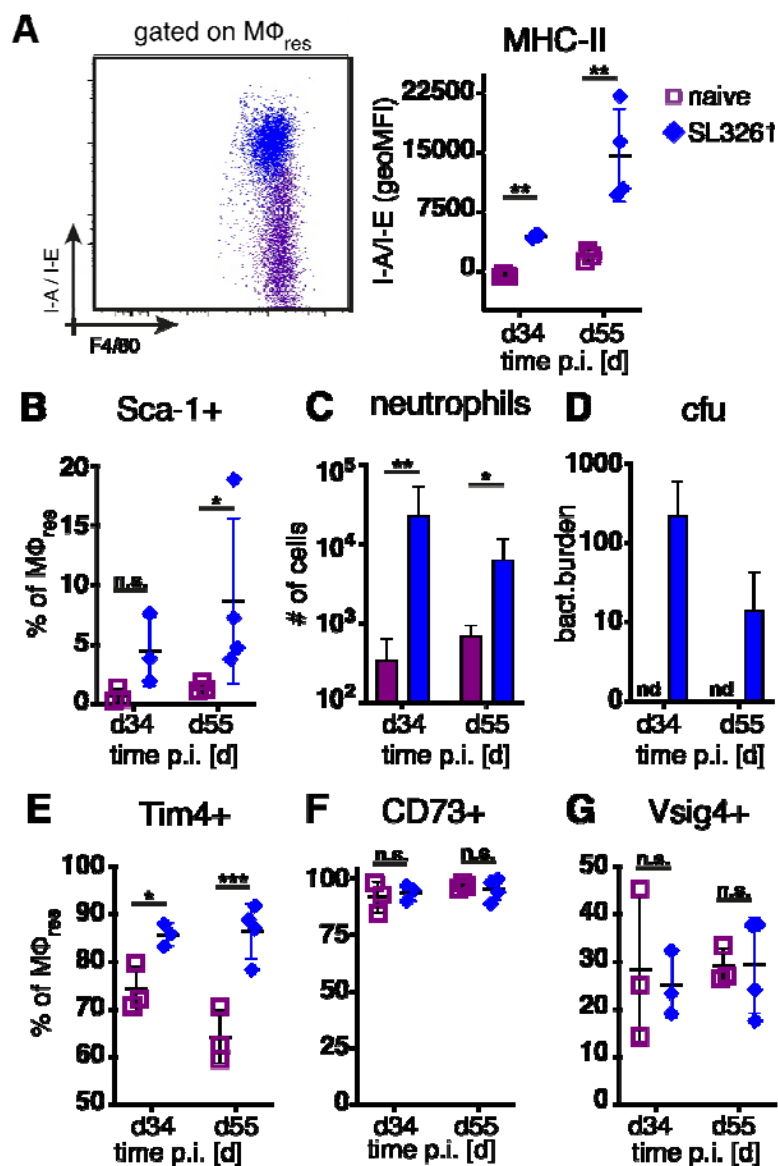


Figure 4

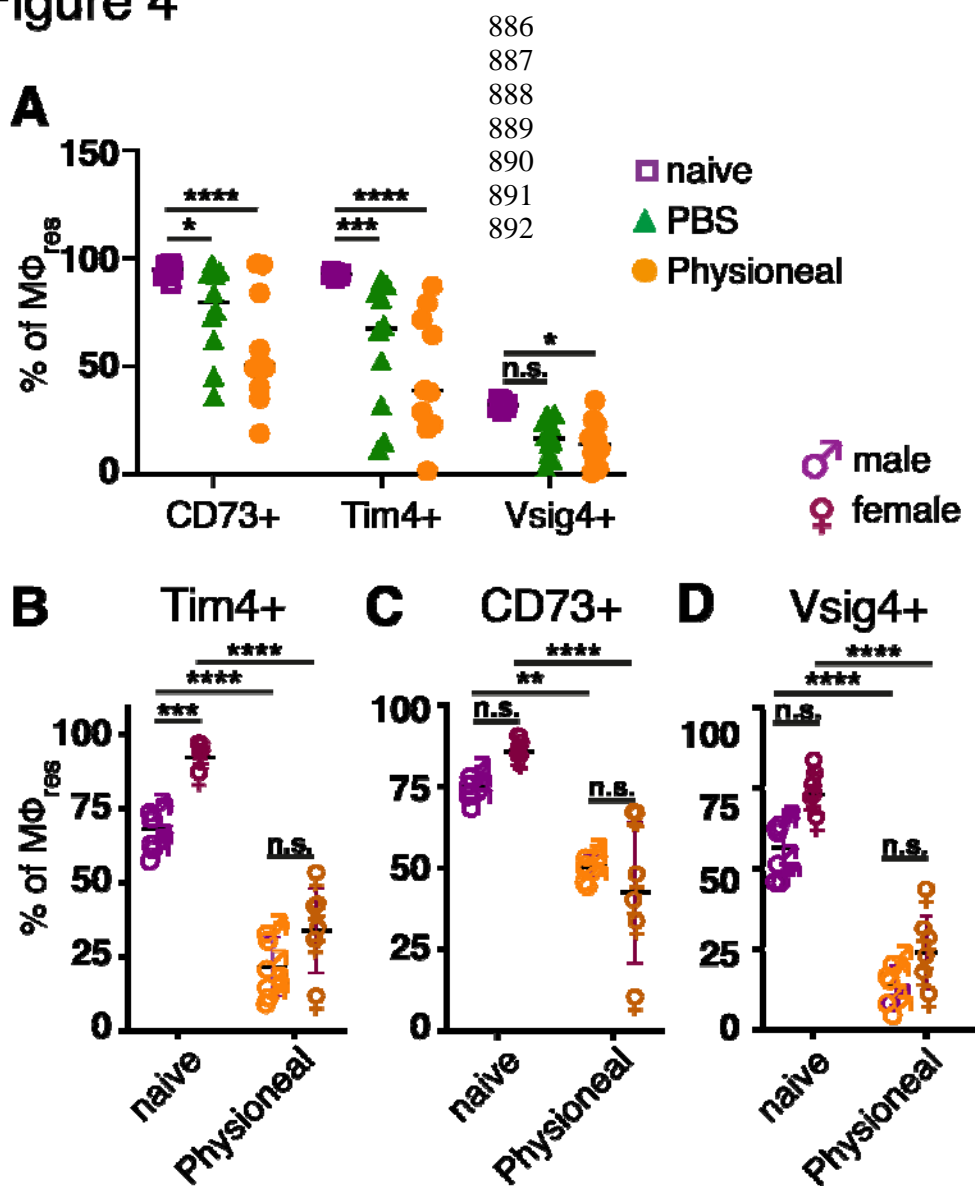


Figure 5

893

894

895

896

897

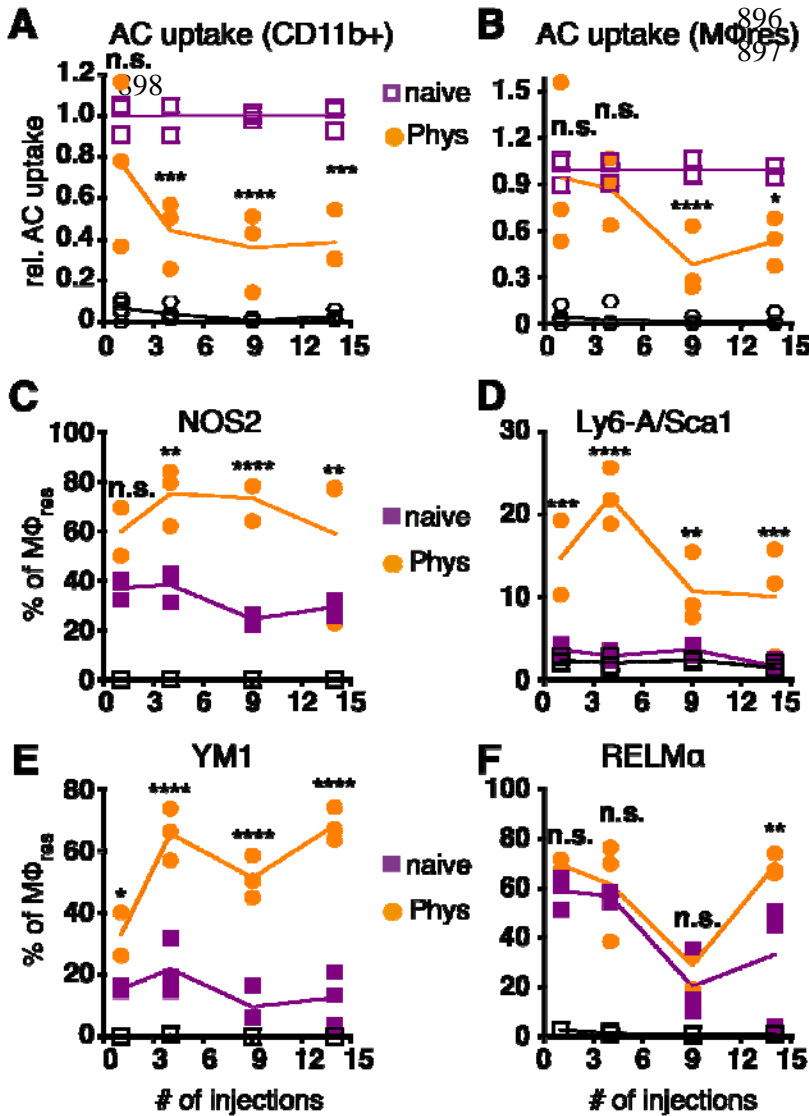


Figure 6

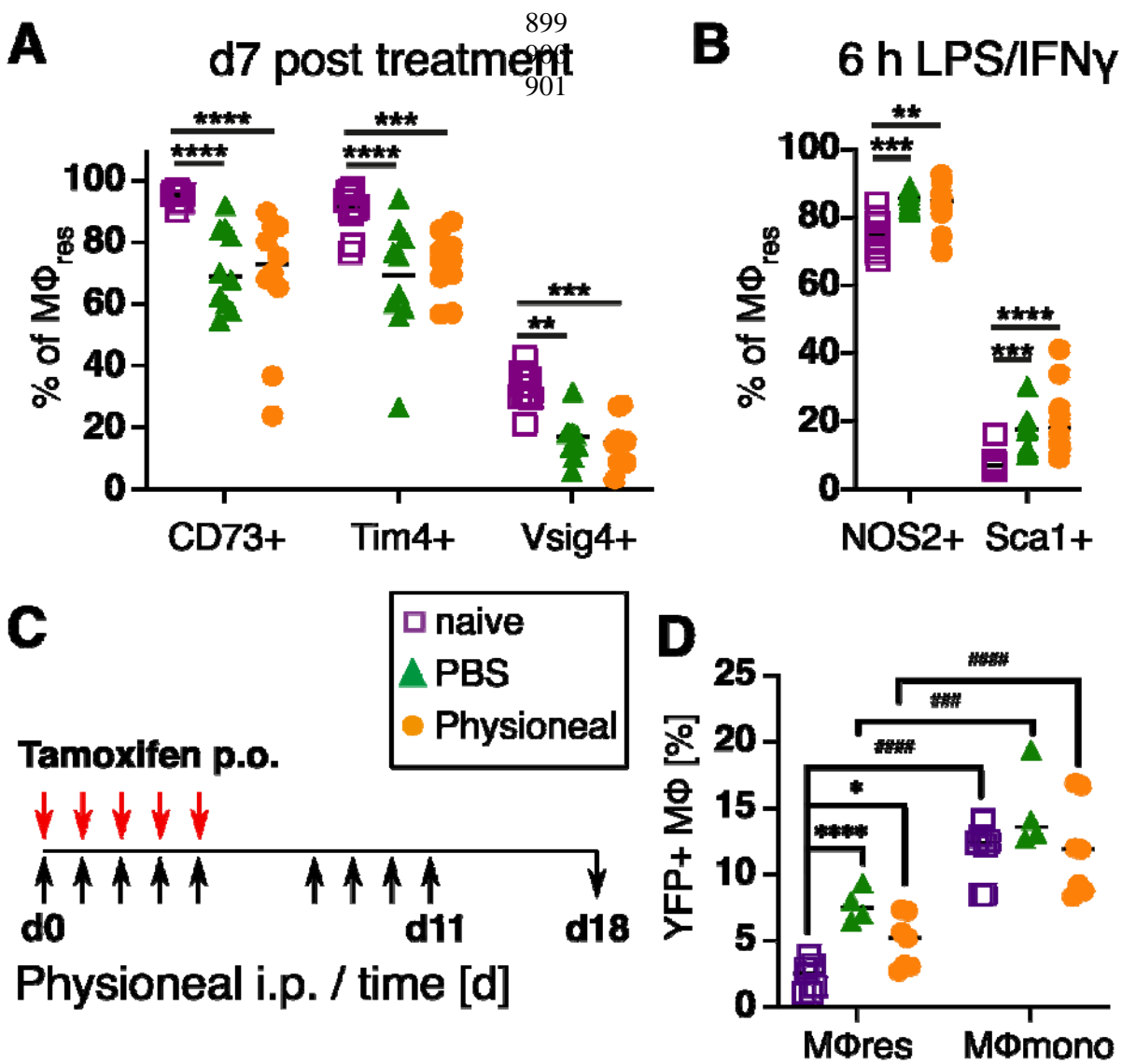
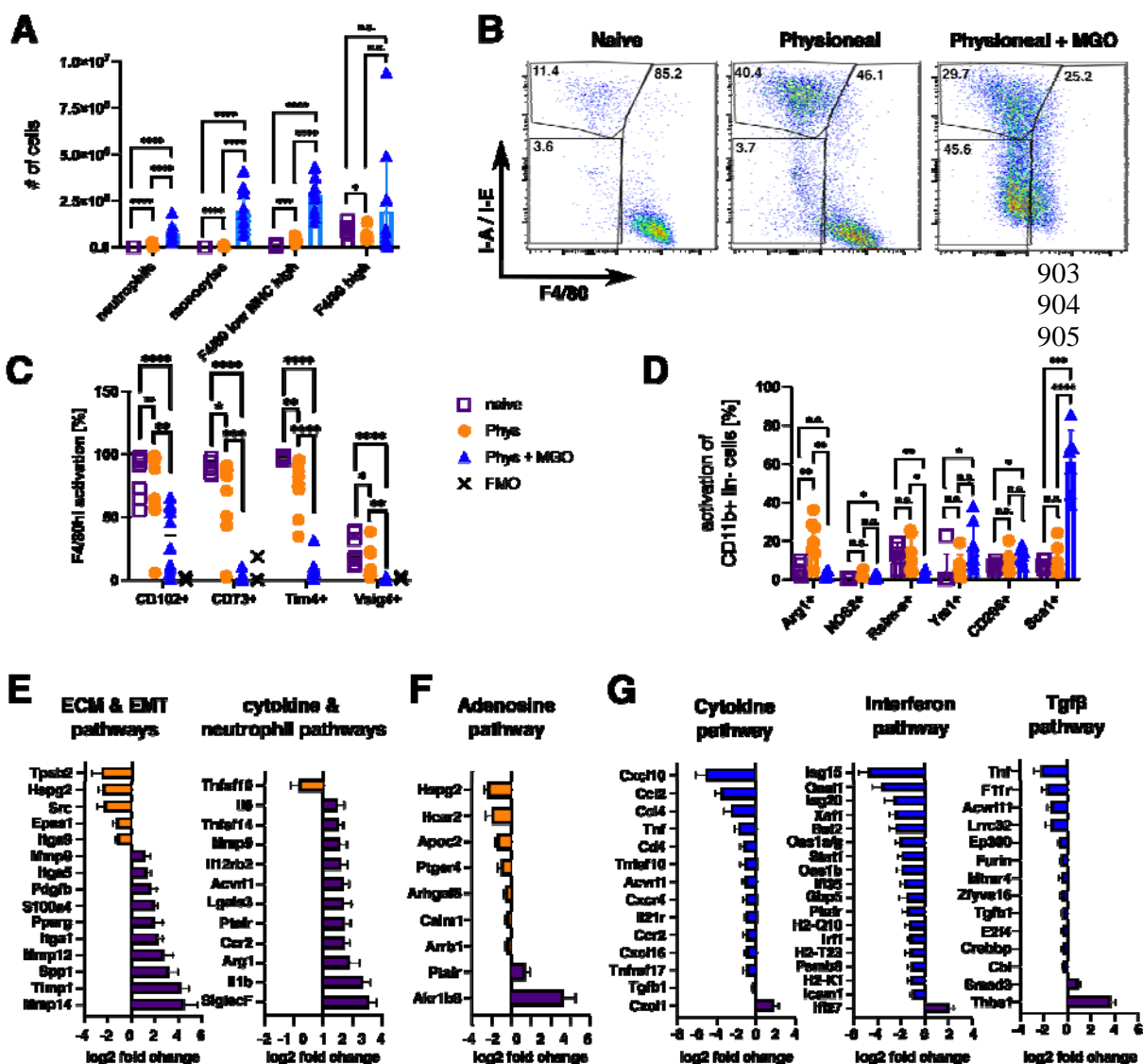
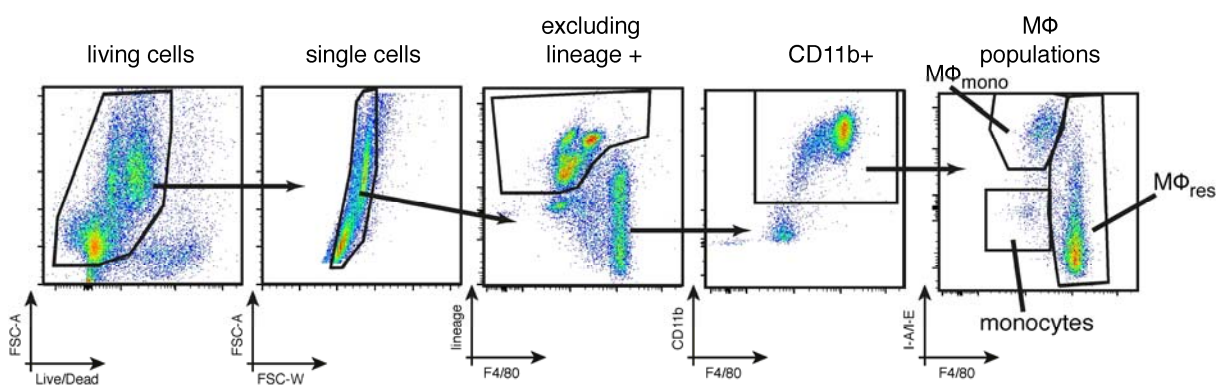


Figure 7

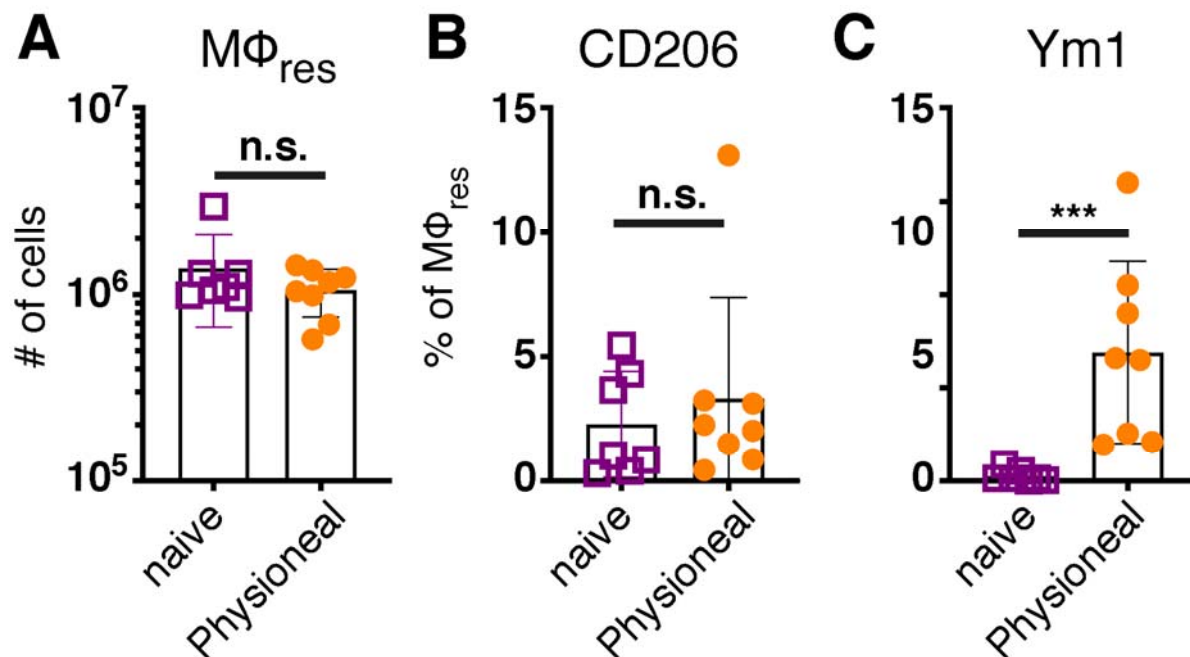
902





Supplementary Figure S1

Figure S1: Gating strategy employed to identify $M\Phi_{res}$, $M\Phi_{mono}$ and Ly6C high monocytes.

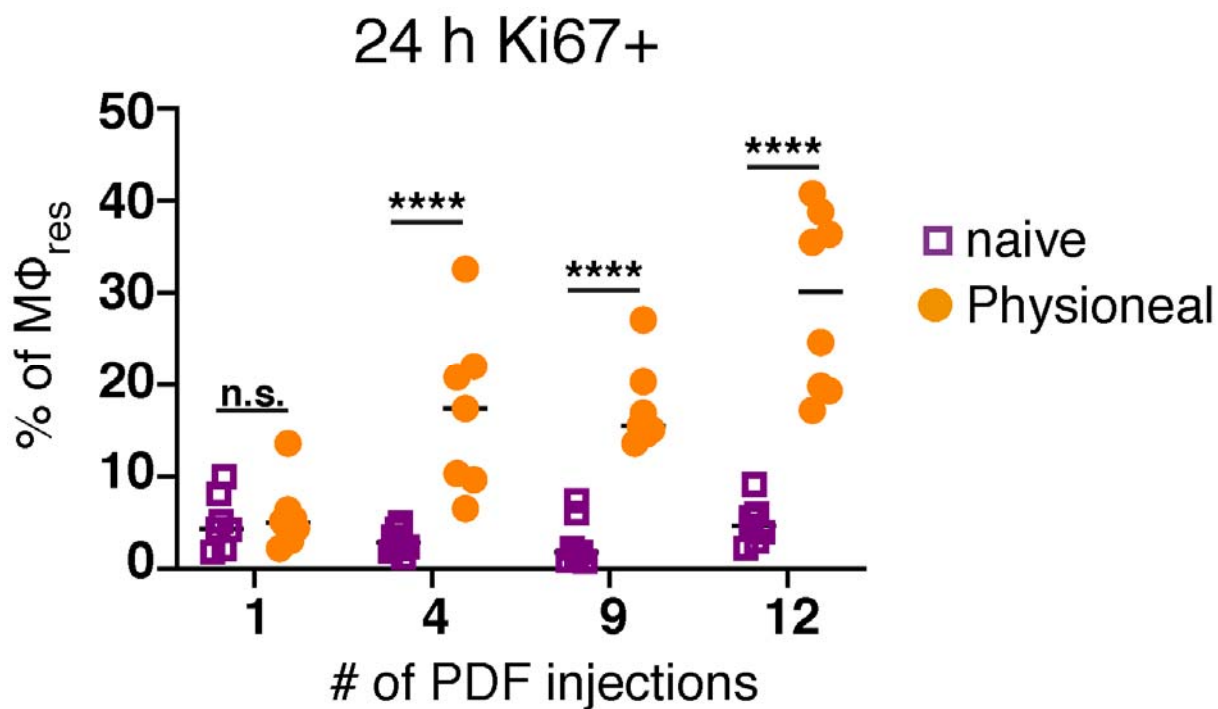


Supplementary Figure S2

Figure S2: The effects of PD fluid injection on peritoneal $M\Phi_{res}$ are transient.

C57BL/6 mice were injected with Physioneal (orange circle) or left untreated (purple square) and whole PEC isolated 24 h p.i.. Cells were analysed by flow cytometry to determine the number of $M\Phi_{res}$ (A) expression of cellular activation markers (B & C).

Datapoints depict individual animals and bars indicate mean and SD. Data pooled from 2 independent experiments using 3-4 animals per group. Data analysed using a Mann-Whitney-U test after transformation. n.s.: not significant; ***: $p < 0.001$



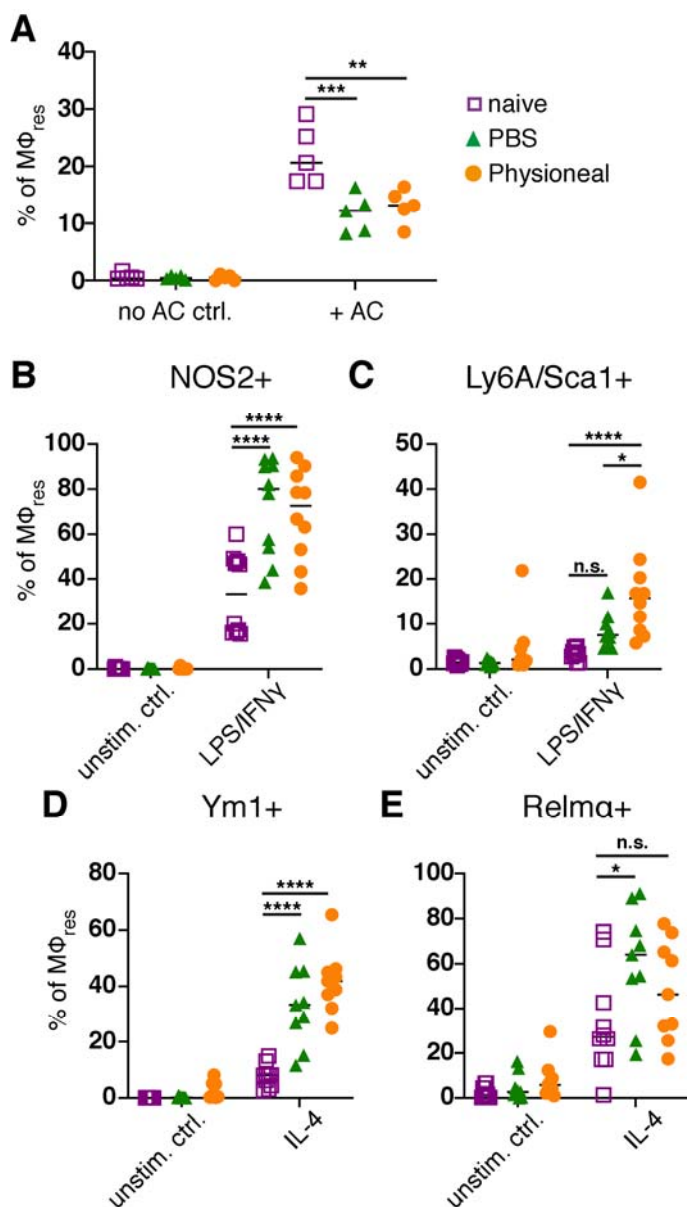
Supplementary Figure S3

Figure S3: MΦ_{res} re-populate the peritoneal cavity through local proliferation following PD fluid injection.

C57BL/6 mice were injected with Physioneal (orange circle) or left untreated (purple square) 5 times a week for the indicated number of injections. At each timepoint whole PEC were isolated 24 h after the last injection and analysed by flow cytometry for intracellular expression of Ki67.

Datapoints depict individual animals and lines indicate mean. Data from separately performed experiments for each timepoint. Data analysed using 2-way ANOVA followed by Sidak's multiple comparison test after transformation.

n.s.: not significant; *: p<0.05; **: p<0.01; ****: p<0.0001



Supplementary Figure S4

Figure S4: Altered MΦ_{res} phenotype is maintained after discontinuation of PD fluid injection.

C57BL/6 mice were injected 5 times a week for a total of nine injections with Physioneal (orange circles), sterile PBS (green triangles) or left untreated (purple squares). 24 h after the last injection whole PEC were isolated and stimulated in vitro with (A) pHRodo labelled apoptotic cells for 90 minutes, (B) LPS/IFN γ for 6 h or (C) IL-4 for 24 h and analysed by flow cytometry.

Datapoints depict individual animals and lines indicate mean. Data pooled from two independent experiments. Data analysed using 2-way ANOVA followed by Tukey's multiple comparison test after transformation. n.s.: not significant; *: p<0.05; **: p<0.01; ****: p<0.0001; #####: P<0.0001

Supplementary Figure S5

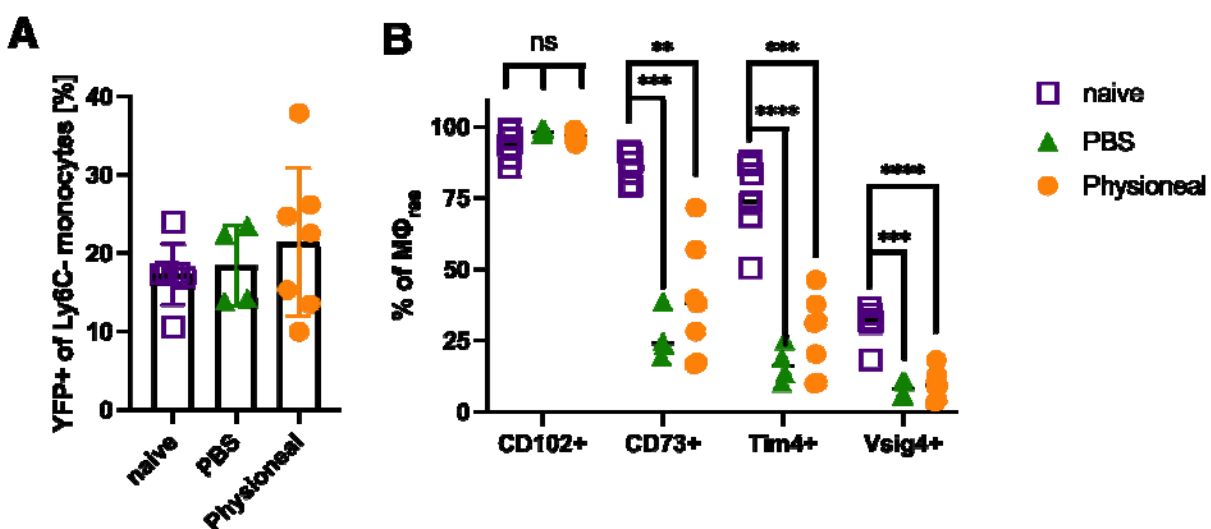


Figure S5: $Cx3cr1^{CreER}:R26-eyfp$ mice were injected daily with 5 mg tamoxifen for 5 consecutive days. Simultaneously, animals received daily injections, five times a week for a total of 9 injections of dialysis fluid (Physioneal, orange circles), PBS (green triangles) i.p. or were left untreated (naive, purple squares). A) Percent eYFP positive, Ly6C- monocytes (CD115+ CD19-) in the blood. B) Expression of CD102, CD73, Tim4 and Vsig4 on peritoneal MΦ_{res} in the mice analysed in A.